# Green Synthesis of $Fe_3O_4$/ZnO Nanocomposite Using *Vernonia amygdalina* Leaf Extract for Antibacterial Applications

**Helen Fisseha Berhe**

**Thesis Submitted to the Department of Applied Chemistry**

**College of Applied Natural Science**

**Presented in Partial Fulfillment of the Requirement for the Degree of Master of Science in Applied Chemistry (Analytical Chemistry)**

**Office of Graduate Studies**

**Adama Science and Technology University (ASTU)**

**May, 2025**

**Adama, Ethiopia**

# Green Synthesis of $Fe_3O_4$/ZnO Nanocomposite Using *Vernonia amygdalina* Leaf Extract for Antibacterial Applications

**Helen Fisseha Berhe**

**Advisor: Hizkeal Tsade (PhD)**

**Thesis Submitted to the Department of Applied Chemistry**
**College of Applied Natural Science**
**Presented in Partial Fulfillment of the Requirement for the Degree of**
**Master of Science in Applied Chemistry (Analytical Chemistry)**

**Office of Graduate Studies**
**Adama Science and Technology University (ASTU)**

**May, 2025**
**Adama, Ethiopia**

# DECLARATION

I hereby declare that this master thesis entitled "**Green Synthesis of $Fe_3O_4$/ZnO Nanocomposite Using *Vernonia amygdalina* Leaf Extract for Antibacterial Applications**" is my own original work. It has not been submitted for the award of any academic degree, diploma, or certificate in any other University. All sources of materials that are used for this thesis have been duly acknowledged through citation.

**Helen Fisseha Berhe**

| | | |
|---|---|---|
| _____ | _____ | _____ |
| **Name of student** | **Signature** | **Date** |

# RECOMMENDATION OF ADVISORS/ SUPERVISORS

I, the major advisor/supervisor of this thesis was, hereby certify that I have closely advised/supervised the student while developing this research and read the draft of dissertation entitled "**Green Synthesis of $Fe_3O_4$/ZnO Nanocomposite Using *Vernonia amygdalina* Leaf Extract fo Antibacterial Applications**" prepared under my guidance by Helen Fisseha Berhe. Therefore, I recommend the submission of the thesis to the department for further review and evaluation.

Dr. **Hizkeal Tsade**

| _____ | _____ | _____ |
|---|---|---|
| Major Advisor | Signature | Date |

## APPROVAL SHEET

I, the advisors of the thesis entitled "**Green Synthesis of $Fe_3O_4$/ZnO Nanocomposite Using *Vernonia amygdalina* Leaf Extract for Antibacterial Application**" and developed by Helen Fisseha Berhe; hereby certify that the recommendation and suggestions made by the board of examiners are appropriately incorporated into the final version of the thesis.

| | | |
|---|---|---|
| Major Advisor | Signature | Date |
| Co-advisor | Signature | Date |

We, the undersigned, members of the Board of Examiners of the thesis by Helen Fisseha Berha have read and evaluated the thesis entitled "**Biogenic Synthesis of Iron Oxide/Zinc Oxide ($Fe_3O_4$/ZnO) Nanocomposite using *Vernonia Amygdalina* Leaves Extract as Reducing Agent for Antibacterial Activity**" and examined the candidate during open defense. This is, therefore, to certify that the thesis is accepted for partial fulfillment of the requirement of the degree of Master of Science in Chemistry (Analytical Chemistry)

| | | |
|---|---|---|
| Chairperson | Signature | Date |
| Internal Examiner | Signature | Date |
| External Examiner | Signature | Date |

Final approval and acceptance of the thesis is contingent upon the submission of its final copy to the Office of Postgraduate Studies (OPGS) through the Department Graduate Council (DGC) and College Graduate Committee (CGC).

| | | |
|---|---|---|
| Department Head | Signature | Date |
| College Dean | Signature | Date |
| Office of Postgraduate Studies, Dean | Signature | Date |

# ACKNOWLEDGEMENT

First I would like to thank the almighty God who gave me the strength and wisdom to complete my work successfully. Then I would like to express my genuine heartfelt gratitude to my advisor, Dr. **Hizkeal Tsade** for his invaluable suggestion, comments, corrections, and professional and technical guidance throughout my work for the successful accomplishment of this thesis. Generally I would like to acknowledge all friends and family to supported material, ideas and who encourages me to continue my study. I would like to express my thanks to the Department of Applied Chemistry, Adama Science and Technology University (ASTU), for providing the necessary knowledge, assistance, and facilities to conduct my research

TABLE OF CONTENTS

Contents page

APPROVAL SHEET ..... III

ACKNOWLEDGEMENT ..... IV

LIST OF TABLES ..... VII

LIST OF FIGURE ..... VIII

LIST OF ABBREVIATION ..... IX

ABSTRACT ..... X

1. INTRODUCTION ..... 1

1.1. Background of the Study ..... 1

1.2. Statement of the Problem ..... 3

1.3. Objective of the Study ..... 3

1.3.1. General objective ..... 3

1.3.2. Specific objectives ..... 3

1.4. Significance of the Study ..... 4

1.5. The scope of the Study ..... 4

2. LITERATURE REVIEW ..... 5

2.1. Nanotechnology ..... 5

2.2. Nanomaterial ..... 5

2.3. Nanoparticles ..... 5

2.4. Synthesis of ZnO Nanoparticles ..... 9

2.4.1. Physical Method ..... 10

2.4.2. Chemical Method ..... 10

2.4.3. Biological /Green Synthesis Method ..... 11

2.5. Synthesis of Magnetic ZnO/$Fe_3O_4$Composite Nanostructures ..... 12

2.5.1. Preparation of Individual Precursors ..... 12

2.6. Plant-Based Green Synthesis of Nanoparticles ..... 14

2.7.Vernonia amygdalina (V.A) plant ..... 15

3. MATERIALS AND METHODS ..... 18

3.1. Chemicals and Reagents ..... 18

3.2. Apparatus and Instruments ..... 18

3.3. Preparation of *Vernonia Amygdalina* leaves ..... 18

3.4. Nanomaterials synthesis ..... 18
3.4.1. Biogenic Synthesis of Fe3O4 ..... 18
3.4.2. Synthesis of ZnO NPs ..... 19
3.4.3. Biogenic Synthesis of $Fe_3O_4$/ZnO NCs ..... 19
3.5. Characterization of $Fe_3O_4$ /ZnO Nano composite ..... 20
3.6. Antibacterial investigation of ZnO NPs, $Fe_3O_4$, and $Fe_3O_4$@ ZnO NCs ..... 20
3.7. Media Preparation and Bacterial Culture ..... 20
3.8. Disc Diffusion Method ..... 20
4. RESULTS AND DISCUSSIONS ..... 22
4.1 UV–Vis Diffuse Reflectance Spectroscopy (DRS) Analysis ..... 22
4.2 X-ray Diffraction (XRD) Analysis ..... 24
4.1. Fourier Transform Infrared Spectroscopy (FTIR) Analysis ..... 26
4.4. Scanning Electron Microscopy (SEM) Analysis ..... 28
4.5.1. Antibacterial Activity of ZnO NPs, $Fe_3O_4$NPs, and $Fe_3O_4$@ZnO Ncs ..... 30
4.5.2. Properties and Antibacterial Mechanisms of ZnO Nanoparticles ..... 31
4.5.3. Mechanisms of Antibacterial Action ..... 31
4.5.4. Antibacterial Properties of $Fe_3O_4$ Nanoparticles ..... 31
4.5.5. Mechanisms of Antibacterial Action ..... 32
4.5.6. Antibacterial Activity of $Fe_3O_4$@ ZnO Nanocomposites ..... 32
4.5.7. Disk Diffusion Methods ..... 33
5. CONCLUSION and RECOMMENDATION ..... 36
5.1. Conclusion ..... 37
5.2 Recommendation ..... 37
REFERENCES ..... 38

# LIST OF TABLES

Table 1.Taxonomic classification of *Vernonia amygdalina* plant ..... 15

Table 2. XRD data of synthesized ZnO NPs, $Fe_3O_4$ NPs, and $Fe_3O_4$/ZnO NCs ..... 26

Table 3. Antibacterial Activity of ZnO NPs, $Fe_3O_4$ NPs, and $Fe_3O_4$@ ZnO Nanocom posite: Inhibition zone diameters (mm) at different concentrations ..... 34

## LIST OF FIGURE

Figure 1.Nanoparticles-classification ..... 7
Figure 2 .Various methods for the preparation of nanoparticles ..... 7
Figure 3.Synthesis of $Fe_3O_4$ Nanoparticles ..... 12
Figure 4. Green synthesis of nanoparticles using plant extract, ..... 15
Figure 5. *Vernonia amygdalina* plant ..... 17
Figure 6. Synthesis approach of $Fe_3O_4$/ZnO NCs ..... 19
Figure 7**.** UV–Vis diffuse reflectance spectra (DRS) and Tauc plots of **(a)** ZnO NPs, **(b)** $Fe_3O_4$ NPs, and **(c)** $Fe_3O_4$@ZnO nanocomposite, their optical absorption and band gap energies. ..... 24
Figure 8. XRD patterns of ZnO NPs (a), $Fe_3O_4$ NPs (b), and $Fe_3O_4$@ZnO nanocomposite (c) ..... 25
Figure 9. FTIR Spectra of **(a)** *Vernonia amygdalina* Leaf Extract, **(b)** ZnO Nanoparticles,**(c)** $Fe_3O_4$ Nanoparticles, and **(d)** $Fe_3O_4$@ZnO Nanocomposite. ... 28
Figure 10.**(a-c)** SEM micrographs of ZnO NPs, $Fe_3O_4$ NPs, and $Fe_3O_4$/ZnO nanocom posite, and **(d)** particle size distribution histograms of $Fe_3O_4$/ZnO nanocomposite ..... 30
Figure 11. Photographs of antibacterial activities of **(a)** ZnO NPs,**(b)** $Fe_3O_4$ NPs, **(c)** ZnO-$Fe_3O_4$ NCs ..... 34

# LIST OF ABBREVIATION

| | |
|---|---|
| E. *coli* | *Escherichia coli* |
| FT-IR | Fourier Transform Infrared Spectrophotometry |
| NCs | Nanocomposites |
| NPs | Nanoparticles |
| UV | Ultraviolet |
| UV-Vis | Ultraviolet Visible Spectrometer |
| XRD | X-ray Diffractometer |
| *P. aeruginosa* | *Pseudomonas aeruginosa* |
| ROS | Reactive Oxygen Species |
| *S.aureus* | *Staphylococcus aureus* |
| SEM | Scanning Electron Microscopy |
| S. *pyogen* | Streptococcus pyogen |
| ZOI | Zone of Inhibition |

# ABSTRACT

*Green synthesized ZnO/$Fe_3O_4$ composite nanostructures have emerged as promising materials due to their unique combination of magnetic and semiconducting properties. These properties make them suitable for the application of antibacterial activity. Thus, the study was focused on the synthesis, characterization, and antibacterial properties of ZnO nanoparticles (NPs), $Fe_3O_4$ NPs, and their resulting $Fe_3O_4$@ZnO nanocomposite. The synthesized materials were characterized by using the modern instrumental techniques including x-ray diffraction (XRD), Fourier transforms infrared (FT-IR), and scanning electron microscope (SEM). The crystalline structure of the materials, with ZnO displaying a hexagonal wurtzite structure and $Fe_3O_4$ exhibiting an inverse spinel structure confirmed by X-ray diffraction (XRD). The nanocomposite presented combined peaks from both ZnO and $Fe_3O_4$, indicating the coexistence of both phases and a smaller crystallite size compared to $Fe_3O_4$ NPs. Followed, the characterized materials was tested for the antibacterial performance against Escherichia coli, Pseudomonas aeruginosa, Staphylococcus aureus, and Streptococcus pyogenes. Findings confirmed that the $Fe_3O_4$@ZnO nanocomposite sowed superior antibacterial activity compared to individual NPs, as evidenced by larger inhibition zones in diffusion experiments. The enhanced antibacterial activity is attributed to the synergistic effects of ZnO and $Fe_3O_4$, including increased Reactive Oxygen Species (ROS) generation and improved stability. Disk diffusion assays assured the greater effectiveness of the nanocomposite against a range of bacterial strains. The improved performance of the nanocomposite is likely due to the combined antimicrobial mechanisms of $Fe_3O_4$@ZnO nanocomposites. These findings highlight the potential of the $Fe_3O_4$@ZnO nanocomposite as a promising candidate for diverse antibacterial applications.*

**Keywords**; Biogenic synthesis, Nanocomposite, *Vernonia Amygdalina* leaves extract, ($Fe_3O_4$/ZnO), Antibacterial Activity.

# 1. INTRODUCTION

## 1.1. Background of the study

Antimicrobial resistance (AMR) has become a significant global health concern due to the reduced effectiveness of conventional antimicrobial agents against resistant microorganisms. This has prompted extensive research on the development of novel antimicrobial materials. Nanocomposites, which combine the unique properties of multiple nanomaterials, have gained attention as potential candidates for combating AMR (Iravani & Varma, 2020)

Currently, nanotechnology is the most advanced and emerging field over all the world. It encircles the application and production of nanoscale material in biological, chemical and physical systems. It involves synthesis, characterization and application of nanoparticles by controlling shape and size. Nanotechnology has recently sparked tremendous research, with applications in science, engineering, agriculture, biotechnology, food science, environment, energy, electronics, space industry, medicine, and biology (Al-Rajhi et al., 2024)

Nanomaterials are particles which can be in nanoscale length, and they are very small particles with advanced thermal conductivity, catalytic reactivity, nonlinear optical performance, and chemical balance because of their big surface area-to-volume ratio. Nanoscale materials are defined as a set of substances where at least one dimension is less than approximately 100 nano meters.(Tripathy & Kim, 2018)

Nanostructures, which are the basic elements of nanoscience and nanotechnology, have come to the fore as important engineering materials in composite, semiconductor,photo catalytic,magnetic, metal oxide, and biomedical applications with their structural, physical, chemical, and biological properties. Metallic based nanostructures have received intense attention from both scientific and industrial community (Ulya & Taufiq, n.d.2024)

Metallic or metal oxide nanostructures have been extensively studied in recent years due to their specific surface area and crystallinity. Among metal oxide nanostructures,

ZnO NPs, as a new type of the low-cost and low-toxicity nanocomposites, have attracted tremendous interest in various biomedical fields, including anticancer, antibacterial, anti-oxidant, anti-diabetic, and anti-inflammatory activities, as well as for drug delivery and bio imaging applications (U. Ali, 2020).

Iron-based magnetic nanoparticles, especially $Fe_3O_4$ as another important metal oxide, are important materials used in ceramics, catalysis, magnetic information storage, medical imaging, drug delivery, biomedical applications, and various electronic applications with their natural magnetic properties. Thus, thanks to the unique and compatible properties of their structures, $Fe_3O_4$ and ZnO allow the production of a higher performance hybrid or composite nanostructures in future applications. Previously, ZnO/$Fe_3O_4$ nanocomposite was synthesized by using sol-gel (Ulya & Taufiq, n.d.) ፣ co-precipitation (Ulya & Taufiq, n.d.), deposition (Kumar et al., 2018) wet milling (Machovsky et al., 2012) microwave assisted(Mousavi et al., 2020) , and wet chemical (Kumar et al., 2018) methods.

Biogenic synthesis involves the use of natural sources, such as plant extracts, as reducing and stabilizing agents in the synthesis of nanomaterials.Furthermore, Biogenic synthesis of this material was made using plant leaves extract as reducing agents instead of chemicals due to the toxic effects of chemicals.This approach offers several advantages, including eco-friendly, cost-effectiveness, and the potential to produce nanomaterials with unique properties (Machovsky et al., 2012) . The use of *Vernonia Amygdalina* leaves extract as a reducing agent in the synthesis of ($Fe_3O_4$/ZnO) nanocomposites provides a sustainable and green alternative to traditional chemical reducing agents.

*Vernonia Amygdalina,* commonly known as bitter leaf, is a medicinal plant with a long history of use in traditional medicine. It is known for its antimicrobial properties attributed to the presence of bioactive compounds such as flavonoids, alkaloids, and terpenoids. These compounds exhibit antimicrobial activity against various pathogenic microorganisms, including bacteria and fungi.

The Biogenic synthesis of ($Fe_3O_4$/ZnO) Nanocomposite using Vernonia A*mygdalinaleaves* extract as a reducing agent is expected to enhance the antimicrobial activity, owing to the presence of bioactive compounds with inherent antimicrobial properties of the Nanocomposite. The synergistic effects of $Fe_3O_4$ and ZnO nanoparticles can lead to improved antimicrobial efficacy, making the nanocomposites a potential candidate for combating AMR (Machovsky et al., 2012).

Therefore, the crystal structure, phase, particle size, functional group, optical properties, thermal stability and morphology of synthesized product were investigated by the standard characterization techniques like FTIR, XRD, SEM and UV-Vis. Thus, the bio synthesized $Fe_3O_4$/ZnO Nanocomposite had been investigated for the application of antimicrobial activities (Roychowdhury et al., 2013).

## 1.2. Statement of the Problem

The growing threat of antimicrobial resistance has significantly reduced the effectiveness of conventional antimicrobial agents, creating an urgent need for alternative therapeutic strategies. Nanocomposites, such as $Fe_3O_4$/ZnO, have emerged as promising candidates due to their enhanced antimicrobial properties. In Ethiopia, the abundant availability of medicinal plants presents a valuable opportunity for the green synthesis of such nanomaterials. Despite this potential, there remains a lack of research on the biogenic synthesis of $Fe_3O_4$/ZnO nanocomposites using locally available medicinal plants, particularly *Vernonia amygdalina*. Infarct, today there is no studies have been reported on the synthesis and antimicrobial evaluation of $Fe_3O_4$/ZnO. nanocomposites derived from *Vernonia amygdalina* leaf extract. This gap highlights the need for an eco-friendly, cost-effective, and efficient approach to synthesize and evaluate such nanocomposites for their antimicrobial potential.

## 1.3. Objective of the study

### 1.3.1. General objective

This study aims to synthesize and characterize $Fe_3O_4$/ZnO nanocomposites using aqueous *Vernonia amygdalina* leaf extract, and to evaluate their antimicrobial activity.

### 1.3.2. Specific objectives

- To synthesize iron oxide/zinc oxide ($Fe_3O_4$/ZnO) nanocomposites (NCs) using *Vernonia Amygdalina* leaves extract as a reducing agent.
- To Characterize the synthesized iron oxide/zinc oxide ($Fe_3O_4$/ZnO) nanocomposites using various techniques such as FTIR, XRD, SEM, and Ultraviolet-Visible (UV-Vis) spectroscopy.
- To investigate the antibacterial activity of *Vernonia Amygdalina* leaves extract-mediated synthesized iron oxide/zinc oxide ($Fe_3O_4$/ZnO) NCs.
- To Compare the antimicrobial activity of the iron oxide/zinc oxide ($Fe_3O_4$/ZnO) NCs with individual $Fe_3O_4$ and ZnO NPs

## 1.4. Significance of the Study

Green synthesis of nanoparticles, rooted in nanobiotechnology, has emerged as a central focus in nanotechnology research. This biosynthetic approach is particularly valued for being environmentally friendly, cost-effective, versatile, and often carried out under mild conditions such as room temperature. It holds significant promise in addressing global challenges, including antimicrobial resistance and the urgent need for sustainable antimicrobial agents.

Antibiotic resistance has diminished the effectiveness of many conventional drugs, underscoring the necessity of exploring alternative antimicrobial strategies. In response, this study presents a novel approach by employing *Vernonia amygdalina* leaf extract rich in bioactive compounds as a green and eco-friendly reducing agent for the synthesis of $Fe_3O_4$/ZnO nanocomposites. These nanocomposites are expected to demonstrate enhanced antimicrobial activity against a broad spectrum of microorganisms, including bacteria and fungi.

By leveraging the inherent antimicrobial properties of *Vernonia amygdalina*, this research contributes to the development of sustainable, cost-effective, and environmentally friendly antimicrobial materials. The findings have potential applications in healthcare, agriculture, and food safety sectors where the demand for effective antimicrobial agents is particularly high.

Ultimately, this study aims to advance innovative, green antimicrobial strategies capable of combating antibiotic resistance and improving public health outcomes. The significance of this research lies in its potential to offer sustainable antimicrobial solutions derived from natural resources, contribute to biomedical innovations, and support progress in the fields of nanotechnology and materials science.

## 1.5. The scope of the study

The scope of this study was limited to synthesis of ($Fe_3O_4$ /ZnO) NCs from *Vernonia Amygdalina* leaves extract, characterization of the ($Fe_3O_4$/ZnO) NCs using, FTIR, XRD, SEM, and UV-Vis spectroscopy technique, its application on some selected antimicrobial pathogens activities.

# 2. LITERATURE REVIEW

## 2.1. Nanotechnology

Nanotechnology is a rapidly evolving field focused on the design, production, and manipulation of materials at the nanoscale level (typically between 1–100 nm). At this scale, nanoparticles (NPs) possess significantly larger surface areas compared to their macro-sized counterparts, resulting in enhanced physical, chemical, and biological properties. The primary goal of nanotechnology is to create, characterize, and manipulate nanomaterials for a wide range of applications (Chandekar et al., 2020) .

This technology offers numerous innovative applications, spanning from advanced fabric materials, food processing, and agricultural production to cutting-edge medical techniques (Ahmed et al., 2017). As one of the most dynamic areas of research, nanotechnology integrates multiple disciplines, leveraging the unique properties of nanoscale materials such as a high surface area-to-volume ratio to achieve functionalities not observed in bulk materials (Dwivedi et al., 2021).

## 2.2. Nanomaterial

Nanomaterials are materials with extremely small dimensions, typically having at least one dimension of 100 nanometers (nm) or less. Depending on their structure, they can be classified as nanoscale in one dimension (e.g., surface films), two dimensions (e.g., strands or fibers), or three dimensions (e.g., particles) (Al Rugaie et al., 2022) . Generally, nanomaterials are considered the foundational building blocks of nanotechnology.

Nanomaterials exhibit unique behaviors compared to their bulk counterparts, owing to properties such as size confinement, enhanced surface area, interfacial phenomena, and quantum effects (Rafique et al., 2020). These characteristics result in superior performance in areas like catalysis, tunable photoreactivity, and mechanical strength. Such enhanced properties make nanomaterials essential for a wide range of applications.

One of the most notable uses of nanotechnology is in environmental remediation, where nanomaterials play a significant role in removing pollutants (Mohanan et al., 2020). Industries such as food processing, pharmaceuticals, cosmetics, paints, plastics, paper, textiles, and agriculture often release hazardous organic and biological pollutants. The integration of science and technology at the nanoscale provides a solid foundation for developing effective solutions to these environmental challenges (Sirelkhatim et al., 2015a).

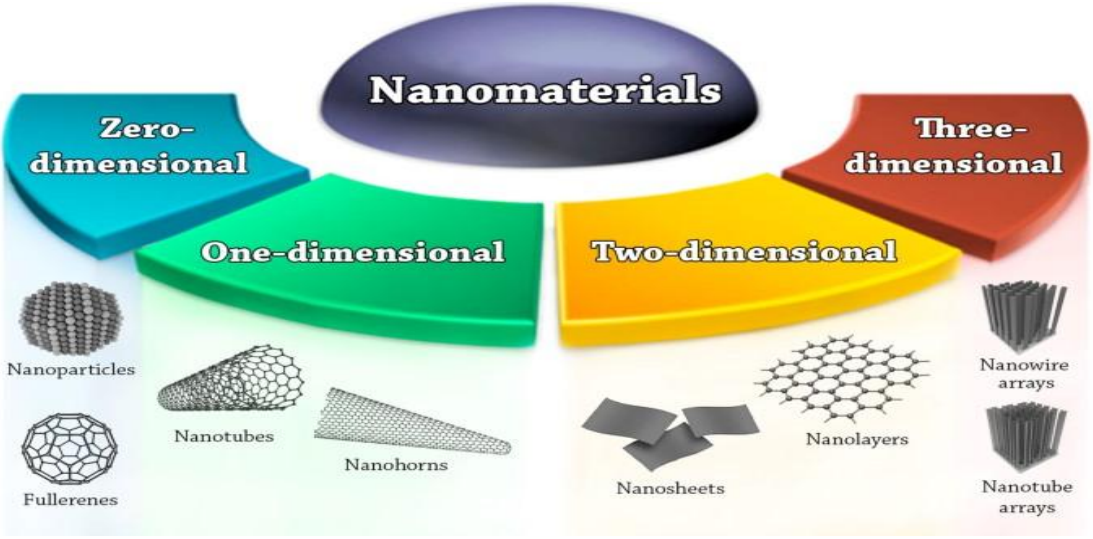


Figure 1.Classification of Nanoparticles

## 2.3. Nanoparticles

The International Organization for Standardization (ISO) defines nanoparticles as nano-objects with all external dimensions in the nanoscale range, where the lengths of the longest and shortest axes do not differ significantly. When the dimensions differ significantly typically by more than a factor of three alternative terms such as nanofibers or nanoplates are preferred over the general term nanoparticles (Lemecho et al., 2022).

Nanoparticles are generally defined as particles ranging in size from 1 to 100 nanometers, and due to their nanoscale dimensions, they often exhibit properties that differ significantly from those of their bulk counterparts. They are utilized across a wide array of applications, including medical treatments, industrial production (e.g., solar cells and oxide fuel batteries for energy storage), and incorporation into consumer products such as cosmetics, textiles, and clothing (Gurunathan et al., 2009)

Nanoparticles can be broadly categorized based on their composition into organic and inorganic types. Organic nanoparticles include materials such as carbon-based nanoparticles (e.g., fullerenes), while inorganic nanoparticles encompass magnetic nanoparticles, noble metal nanoparticles (e.g., gold and silver), and semiconductor nanoparticles (e.g., zinc oxide and titanium dioxide) (Machovsky et al., 2012).

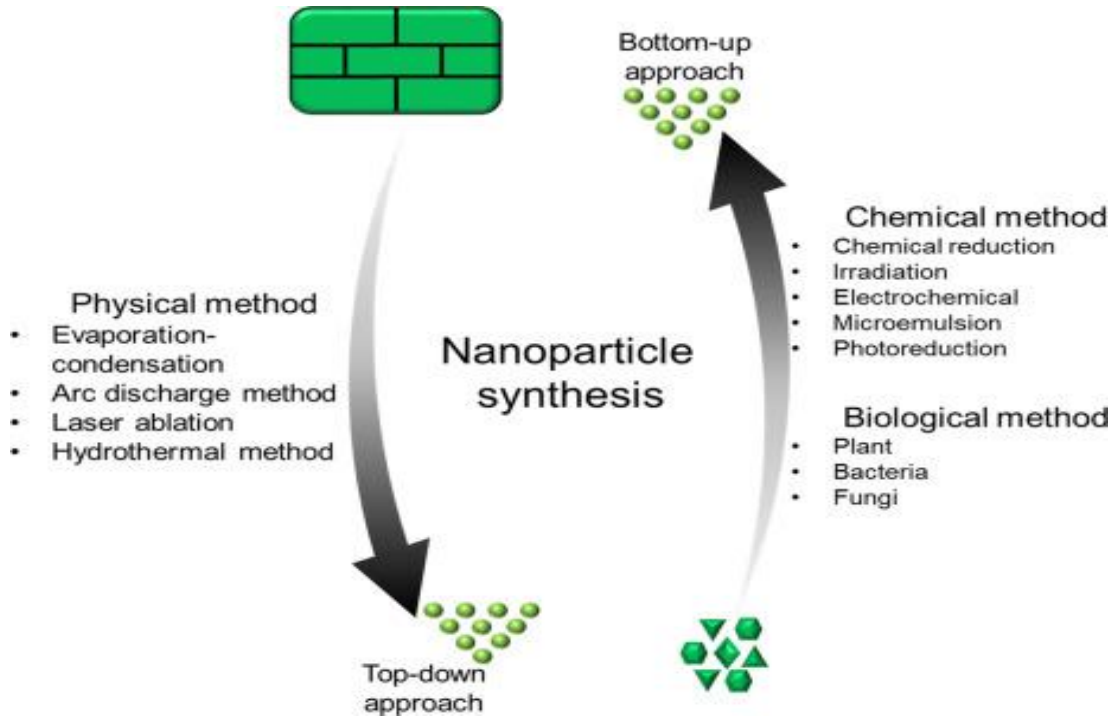


Figure 1 .Various methods for the preparation of nanoparticles

The core methods for nanoparticle (NP) synthesis are generally classified into physical, chemical, and biological approaches. The resulting nanoparticles have a wide range of biomedical applications, including imaging, biosensing, diagnostics, biological therapies, drug delivery, bioconjugation, and hyperthermia treatments (Shell et al., 2010).

Among these, biological synthesis commonly referred to as green synthesis offers several advantages over traditional physical and chemical methods. First, it is relatively simple, energy-efficient, scalable, and requires fewer processing steps (N. Ali et al., 2024). Second, it is environmentally friendly, as it minimizes the use of toxic chemicals and tends to produce safer products and byproducts (Hasan, 2015) . This makes green synthesis especially suitable for use in sensitive fields such as food production, pharmaceuticals, and cosmetics (Uikey, 2016) . In general, nanoparticles synthesized via green methods exhibit lower toxicity, making them more appropriate for biomedical applications (Drug, 2021).

In contrast, physical and chemical methods are often cost-intensive, require high energy input, and involve the use of hazardous chemicals, which may lead to toxic effects on human cells. Green synthesis, however, does not necessarily require high temperatures, pressure, or energy, making it a more sustainable option(P. Singh et al., 2016) . Nonetheless, to achieve consistent and biologically functional nanoparticles, several parameters must be carefully controlled such as pH, chemical concentration, reaction time, and temperature (Drug, 2021).

An additional advantage of plant-based green synthesis over microbial-based systems is that it eliminates the need for maintaining microbial cultures, which reduces costs associated with microorganism isolation and culture media preparation (Parveen et al., 2016) . Plant-derived nanoparticles typically range in size from 1 to 100 nm, although some larger particles up to 500 nm may also be formed (Kuppusamy et al., 2016) Regardless of the synthesis method used, nanoparticles may contain impurities, which are a major cause of cytotoxicity in human cells. These impurities can be removed through dialysis or filtration, ensuring safer application in biological systems (Makarov et al., 2014)

## 2.4. Synthesis of ZnO Nanoparticles

Zinc oxide (ZnO) is a semiconducting inorganic material that exists in three different crystal structures: wurtzite, zinc blende, and rock salt. Under ambient conditions, the wurtzite structure is thermodynamically stable, characterized by each zinc atom being tetrahedrally coordinated with four oxygen atoms. With a wide band gap ranging from 3.1 to 3.3 eV, ZnO exhibits excellent potential for various applications, including biosensors, cosmetics, drug delivery systems, and antibacterial agents (Paper et al., 2016).

ZnO nanoparticles (ZnO NPs) can be synthesized using various methods, including physical, chemical, and biological approaches (Amin et al., 2011). A wide variety of ZnO nanostructures have been successfully synthesized with diverse morphologies such as nanorods, nanospheres, nanotubes, nanowires, nanoneedles, and nanorings. Other complex shapes like spirals, drums, polyhedrons, disks, flowers, stars, boxes, and plates can also be formed by carefully adjusting the growth conditions (N. Ali et al., 2024).

Physical methods for ZnO NP synthesis include radiolysis, sonication, spray pyrolysis, photo-irradiation, electrospinning, and laser ablation. Despite their effectiveness, these methods often require high energy input and specialized equipment. On the other hand, chemical methods such as the sol-gel, solvothermal, co-precipitation, and template-assisted processes have gained more attention due to their better control over particle size and shape (Pramanik et al., 2016).

Among chemical techniques, the sol-gel method is widely used due to its simplicity, low processing temperatures, and ability to produce large quantities of ZnO NPs. Other physical techniques, including vapor deposition, plasma irradiation, and ultrasonic irradiation, are also employed for nanoparticle fabrication (Tippayawat et al., 2016). However, the significant energy requirements and cost of equipment associated with these methods limit their large-scale application.

As an alternative, biological (green) synthesis of ZnO NPs offers a cost-effective, energy-efficient, and environmentally friendly approach. It is easy to perform, requires minimal equipment, and avoids the use of toxic chemicals, making it a highly suitable method for sustainable nanoparticle production (Gul et al., 2024).

### 2.4.1. Physical Method

Physical methods for synthesizing ZnO nanoparticles typically involve a top-down approach and require expensive equipment, high temperatures and pressures, and large installation spaces for machinery (Gul et al., 2024). Common physical techniques include high-energy ball milling, melt mixing, physical vapor deposition (PVD), laser ablation, sputter deposition, arc deposition, and ion implantation. Other widely researched methods include vapor-liquid-solid (VLS), chemical vapor deposition (CVD), and PVD, which are known for producing high-purity nanomaterials.

Among these, the high-energy ball milling method is a cost-effective, efficient, and relatively simple technique for fabricating ZnO nanostructures. It relies on mechanical force to break down bulk material into nanoparticles.

Laser ablation, another physical technique, utilizes a laser beam to remove material from a solid or liquid surface. In this method, pulsed laser ablation is often performed in double-distilled water. At lower reflux conditions, the laser heats and vaporizes the material; under higher reflux, the material is converted into plasma, enabling nanoparticle formation (Agarwal et al., 2017).

Thermal evaporation is also commonly used. This process involves vaporizing powdered starting material and condensing it into nanoparticles under controlled conditions such as temperature, pressure, atmosphere, and substrate (P. Singh et al., 2016). It is considered simple, inexpensive, and non-catalytic. For example, ZnO nanobelt structures have been fabricated via thermal evaporation of oxide powders without using a catalyst (Agarwal et al., 2017).

Despite the advantages of precision and control, physical methods are often resource-intensive, making them less favorable for large-scale, eco-friendly, and cost-sensitive applications compared to biological or green synthesis approaches (I. H. N. B. Singh, 2026).

### 2.4.2. Chemical Method

Chemical synthesis is one of the most widely used techniques for producing nanoparticles and involves the use of various precursors under controlled conditions such as temperature, reaction time, and reactant concentrations. By adjusting these parameters, researchers can effectively control the morphology, size, and shape of the

resulting nanoparticles (Length, 2006). Chemical synthesis methods can be broadly classified into liquid-phase and gas-phase approaches.

Liquid-phase synthesis includes techniques such as precipitation, co-precipitation, colloidal synthesis, sol-gel processing, water-in-oil microemulsion, hydrothermal, solvothermal, sonochemical, and polyol methods.Gas-phase synthesis, on the other hand, involves methods like pyrolysis and inert gas condensation (Al Rugaie et al., 2022).

Despite the versatility and effectiveness of chemical synthesis, each method comes with its own limitations, particularly in terms of nanoparticle stability and the tendency for self-aggregation. These drawbacks can compromise the functional properties and reproducibility of the nanoparticles (Length, 2006).

As a result, there has been a growing shift in recent years toward green synthesis methods, which utilize biological agents such as plant extracts, bacteria, or fungias eco-friendly and sustainable alternatives for synthesizing metal and metal oxide nanoparticles. This approach not only addresses the issues of toxicity and environmental impact but also offers improved biocompatibility for applications in fields such as biomedicine, agriculture, and environmental remediation (Akpomie et al., 2021).

### 2.4.3. Biological /Green Synthesis Method

The term “green synthesis” refers to the use of natural resources, particularly plant extracts, for the fabrication of nanoparticles (Akpomie et al., 2021). Plants serve as primary biological producers capable of synthesizing various metal and metal oxide nanostructures (Lemecho et al., 2022). Compared to microorganisms, plant extracts are considered superior biological agents for nanoparticle synthesis because they are abundant, stable, environmentally friendly, cost-effective, and safe to handle, while also possessing a wide range of metabolic functionalities (Ocimum et al., 2016). Additionally, plant extracts facilitate rapid metal ion reduction and offer better scalability for nanoparticle production. Consequently, much of the current research on nanoparticle biosynthesis focuses on plants, which have consistently demonstrated higher success rates compared to other green synthesis methods (Frey et al., 2025).

Nanoparticle biosynthesis involves the production of nanoparticles using microorganisms and plants, primarily for biomedical applications. Nanoparticles synthesized via biomimetic or green approaches often exhibit enhanced catalytic

activity, while minimizing the need for expensive and toxic chemicals. The green synthesis method is an environmentally friendly, sustainable approach that employs naturally bioavailable and inexpensive resources such as extracts from green plants, algae, fungi, yeasts, bacteria, and viruses to produce stable nanoparticles for a wide variety of applications (P. Singh et al., 2016).

## 2.5. Synthesis of Magnetic ZnO/$Fe_3O_4$Composite Nanostructures

ZnO/$Fe_3O_4$ composite nanostructures have emerged as promising materials due to their unique combination of magnetic and semiconducting properties. These properties make them suitable for various applications, including gas sensing, photo catalysis, magnetic separation, and drug delivery.Here's an overview of the synthesis of ZnO/$Fe_3O_4$ composite nanostructures (Taha Yassin et al., 2024):

### 2.5.1. Preparation of Individual Precursors

$Fe_3O_4$ Nanoparticles: These can be synthesized through various methods, such as cop precipitation, hydrothermal, and sol-gel methods. Typically, iron salts like $FeCl_2$ and $FeCl_3$ are used as precursors.

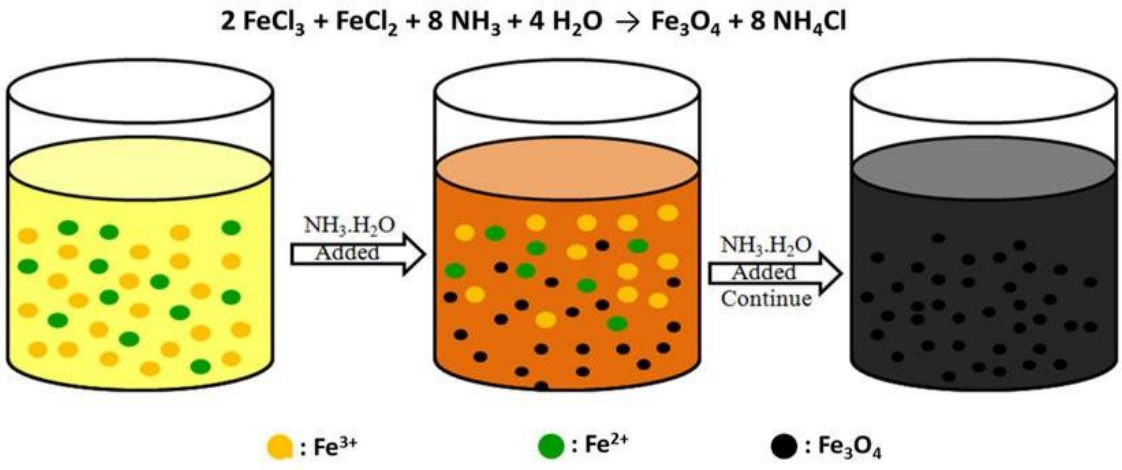


Figure 2. Synthesis of $Fe_3O_4$ Nanoparticles

**ZnO Nanoparticles:** Similar to $Fe_3O_4$, ZnO nanoparticles can be synthesized using various methods like hydrothermal, sol-gel, and precipitation methods. Zinc salts like ZnCl2 and $Zn(NO_3)_2$ are commonly used as precursors (Anuradha & Raji, 2021).

### 2.5.2. Assembly of the Composite

Several methods can be employed to assemble the ZnO and $Fe_3O_4$ nanoparticles into composite nanostructures. Some common techniques include:

Hydrothermal Method: This method involves heating a mixture of the precursors in a sealed container under high pressure and temperature. The controlled growth conditions allow for the formation of well-defined ZnO/$Fe_3O_4$ nanostructures.

Sol-gel Method: This method involves the hydrolysis and condensation of metal alkoxide precursors in a solvent to form a gel. The gel is then dried and calcined to obtain the desired composite nanostructures.

Layer-by-Layer (LBL) Assembly: This technique involves the alternate deposition of oppositely charged layers of ZnO and $Fe_3O_4$ nanoparticles onto a substrate. This method allows for precise control over the thickness and composition of the composite nano structure (Lemecho et al., 2022)

## 2.6. Plant-Based Green Synthesis of Nanoparticles

Green synthesis has gained significant importance as a sustainable, economical, feasible, and environmentally friendly method for producing various bio-inspired nanomaterials. It helps reduce the harmful effects commonly associated with physical and chemical nanoparticle synthesis methods. The phytochemicals present in plants play a crucial role in green synthesis by exhibiting strong reduction and stabilization capabilities. Nanoparticles can be biologically synthesized using a range of organisms including bacteria, fungi, algae, and plants (Anuradha & Raji, 2021) .

Among these, plants have shown the greatest potential for nanoparticle production. Microbial synthesis often faces challenges such as culture contamination, lengthy processes to generate sufficient biomass, limited control over nanoparticle size, and difficulty in reusing biomass for repeated nanoparticle synthesis. Moreover, maintaining microbial cultures under sterile conditions and isolating microorganisms can be costly and time-consuming (Mousavi et al., 2020).

In contrast, plant-based synthesis offers several advantages: high stability of the nanoparticles, lower risk of contamination, simple preparation procedures, and reduced time requirements (Khairy et al., 2024). Plants and their extracts act as natural chemical factories due to the presence of various phytochemicals such as flavonoids, terpenoids, phenols, polyphenols, amides, aldehydes, and saponins (Rafique et al., 2020) . These compounds, along with plant enzymes like reductases, contribute to the reduction of metal ions and capping of nanoparticles, thus stabilizing them.

Using plants eliminates the need for expensive instruments, high-pressure conditions, and hazardous chemicals typically required in other synthesis methods, making green synthesis a safer and more accessible alternative (Sirelkhatim et al., 2015b).

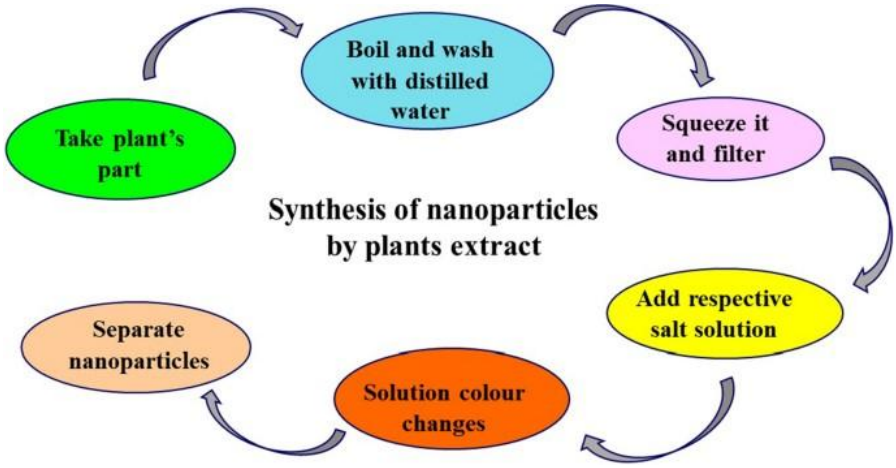


Figure 3. Green synthesis of nanoparticles using plant extract,

## 2.7.*Vernonia amygdalina* (V.A) plant

*Vernonia amygdalina* (commonly known as bitter leaf) is a shrub that predominantly grows in tropical Africa. The leaves of this plant are used both as a food vegetable and as a culinary herb in soups. *Vernonia amygdalina* is a shrub or small tree typically reaching a height of 2-5 meters and belongs to the family Asteraceae. Its leaves are petiolate, approximately 6 mm in diameter, and elliptic in shape. The leaves are green with a characteristic odor and a distinctly bitter taste. The botanical name is *Vernonia amygdalina*, and it is widely referred to as "bitter leaf" in English (Ocimum et al., 2016)

*V. amygdalina* naturally occurs along rivers and lakes, at forest margins, in woodlands, and grasslands up to altitudes of 2800 meters. It thrives in regions with an average annual rainfall between 750 and 2000 mm. The plant requires full sunlight and prefers humid environments. Although it can grow in various soil types, it favors humus-rich soils (Amin et al., 2011).

Table 1.Taxonomic classification of *Vernonia amygdalina* plant

| Scientific Classification of *Vernonia amygdalina* | |
|---|---|
| Kingdom | Plantae |
| Division | Angiosperm |
| Class | Angiospermida |
| Sub-class | *Asteridae* |
| Order | Asterales |
| Family | Asteraceae |
| Genus | Vernonia |
| Specie | *V. amygdalina* |

Vernonia amygdalina is a widely used medicinal plant in West Africa. Its fresh leaves are of great dietary importance due to their rich content of vitamins and mineral salts, making it a valuable protective food. It plays a significant role in maintaining health and is used traditionally for the prevention and treatment of various diseases.

The leaves, in particular, are known for their effectiveness in ethnotherapy for conditions such as diabetes, asthma, headaches, skin infections (e.g., ringworm, rashes, eczema), schistosomiasis, malaria, measles, diarrhea, tuberculosis, abdominal pain, intestinal complaints, fevers, coughs, infertility in women, and hyperlipidemia (Drug, 2021). Bitter leaf also supports the detoxification of vital organs like the liver and kidneys.

As a pharmacologically active plant, *V. amygdalina* contains complex bioactive compounds with anticancer, antibacterial, antimalarial, and antiparasitic properties. In ethnomedicine, both the roots and leaves are used to treat fever, hiccups, kidney issues, and stomach discomfort (N. Ali et al., 2024).

In many West African countries, including Cameroon, Ghana, and Nigeria, the stem and root of *V. amygdalina* are commonly used as chewing sticks (Koshy et al., 2009). Additionally, the plant is traditionally used to promote blood clotting and has been shown to significantly reduce blood glucose levels postprandially. In Northern Nigeria, it is mixed into horse feed to make a tonic known as *Chusar Doki* in Hausa, which serves as a strengthening or fattening agent (Iravani & Varma, 2020).

In Ethiopia, the leaves are used similarly to hops in the preparation of local alcoholic beverages such as tela, beer, and tegi (Ghaem et al., 2019). In Nigeria and other parts of Africa, the leaves are widely used to treat fevers and are considered a quinine substitute (Atla et al., 2018). The young leaves are traditionally employed as anthelmintics, antimalarials, laxatives/purgatives, enemas, expectorants, worm expellers, and fertility inducers in sub-fertile women. Notably, wild chimpanzees in Tanzania have been observed using the plant to treat parasite-related diseases (Geneti et al., 2022).

Moreover, many herbalists and naturopathic practitioners recommend aqueous extracts of *V. amygdalina* for treating emesis, nausea, diabetes, loss of appetite, dysentery, and other gastrointestinal disorders

Figure 4. *Vernonia amygdalina* plant

*Vernonia amygdalina* leaves, also known as bitter leaf, leaf, have been traditionally used for centuries across various cultures due to their medicinal properties. Scientific research has confirmed the presence of numerous bioactive compounds in the leaves, such as terpenoids, flavonoids, and alkaloids, which are responsible for a wide range of therapeutic effects, including notable antimicrobial activity (Bekele et al., 2022).

# 3. MATERIALS AND METHODS

## 3.1. Chemicals and Reagents

Chemicals reagents, and solvents such Sodium hydroxide (NaOH), Hydrochloric acid (HCl), Zinc Nitrate salt $ZnNO_3$), absolute ethanol, Ferric chloride ($FeCl_3.6H_2O$) and ferrous chloride ($FeCl_2$), Muller–Hinton agar, dimethyl sulfoxide (DMSO),and distilled water were used to this research.

## 3.2. Apparatus and Instruments

The necessary apparatus and instruments employed for this research included a polyethylene bag, pH meter, beaker (350-400 mL), volumetric flask (10, 25, 100 mL), measuring cylinder (10 mL), conical flask (250 mL), filter paper, hot plate, magnetic stirrer, centrifuge (3000-6000 rpm), centrifuge tube, crucible dish, aluminum foil, plastic micro tubes, and micro pipette. The instruments included X-ray diffractometer (XRD), scanning electron microscope (SEM), Fourier transform infrared spectroscopy (FTIR), and Ultraviolet-Visible (UV-Vis) Spectroscopy were used.

## 3.3. Preparation of *Vernonia Amygdalina* leaves

The *Vernonia Amygdalina* leaves sample was collected and taken from local area or ASTU Campus. The leaves extract of *Vernonia Amygdalina* leaves was prepared by following the general method as described in. Briefly, the collected fresh leaf of *Vernonia amygdalina* leaves was wash twice with distilled water to remove any surface impurities and dust followed by air-dried at room temperature in shaded region. Then, 20g of dried leaf was grind with pestle and mortar, and the resulting powder was boiled in 400 mL of distilled water using 1000 mL Erlenmeyer flask at 50 $^oC$ for 1 h. The extract was cooled and filters using Whatman filter paper No.(Gul et al., 2024) . Finally, the filtrate was poured in containers and store in refrigerator for further use.

## 3.4. Nanomaterials synthesis

### 3.4.1. Biogenic Synthesis of Fe3O4

$Fe_3O_4$ NPs was synthesized by the procedure adapted from (Machovsky et al., 2012). Briefly, 15 mL of the *Vernonia amygdalina* leaf extract solution was added to 100 mL of an aqueous solution of $FeCl_3$. The black precipitate that formed was isolated by centrifugation (3000 rpm for 30 min), washed with in distilled water, and dried in a

vacuum oven for 3 h. After drying, it was further calcined in a muffle furnace for 3 h. Finally, the biogenically synthesized $Fe_3O_4$ NPs were stored in a glass bottle for further characterization and application, and were named *Vernonia amygdalina* leaves extract of $Fe_3O_4$ NPs.

### 3.4.2. Synthesis of ZnO NPs

ZnO NPs, was synthesized based on general procedure adapted from (Drug, 2021). Briefly, 15 mL of the *Vernonia amygdalina* leaf extract solution was added to 100 mL of an aqueous solution of Zinc acetate [$Zn(O_2CCH_3)_2(H_2O)_2$]. A yellow precipitate formed after mixing and was constantly swirled for 30 minutes at 800 rpm using a magnetic stirrer. The precipitate was periodically cleaned in ethanol and distilled water to get rid of any remaining impurities, and then oven-dried at 100℃ for an hour. Using a blender, the produced dried light yellow-colored powder was obtained for further characterization and applications.

### 3.4.3. Biogenic Synthesis of $Fe_3O_4$/ZnO NCs

The $Fe_3O_4$/ZnO oxide nanocomposite was prepared in a similar manner with a slight modification (Al Rugaie et al., 2022). And 80 mg sample of synthesized $Fe_3O_4$ was dispersed in 50 mL of water by ultra-sonication for 25 min. Subsequently, 100 mL of an aqueous solution of zinc acetate ($(CH_3COO)_2{\cdot}2H_2O$) was added to the dispersed solution. A 10 mL sample of the *Vernonia amygdalina* leaves extract solution was added, and both solutions were mixed and stirred magnetically for 60 min. The obtained brown precipitate was isolated by centrifugation (3000 rpm for 25 min), washed with distilled water, and dried in a vacuum oven for 3 h. After drying, it was further calcined in a muffle furnace for 3 h, Finally, the biogenically synthesized $Fe_3O_4$/ZnO nanocomposite was stored in a glass bottle for further characterization and application.

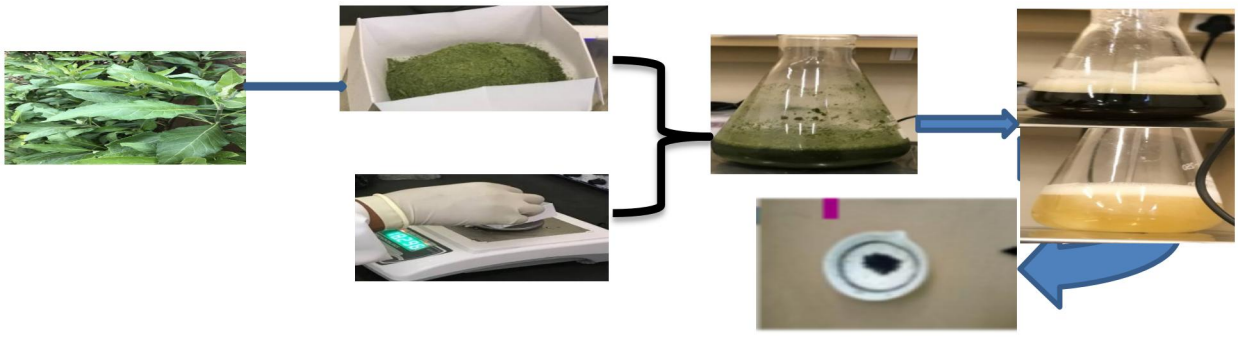

Figure 5. Synthesis approach of $Fe_3O_4$/ZnO NCs

## 3.5. Characterization of $Fe_3O_4$ /ZnO Nano composite

The crystalline size and structure of the synthesized $Fe_3O_4$ /ZnO were investigated by the X-ray diffraction using an X-ray diffractometer at ASTU in Material Science and Engineering Department and The crystallite size of the nanocomposite was calculated by using Debye Scherer's equations Also, the morphology, chemical composition, and crystalline structure of the synthesized of Nano composite was analyzed using scanning electron microscopy SEM, and Phytochemicals found in the leaf extract acted and synthesized nanoparticles/Nano composite were investigated by using FTIR spectrometer in Addis Ababa University at sdst (6) killo. And also the band gap energy of Nano composite was estimated by ultraviolet-visible spectroscopy in ASTU.

### 3.6. Antibacterial investigation of ZnO NPs, $Fe_3O_4$, and $Fe_3O_4$@ ZnO NCs

The antibacterial activity of synthesized ZnO NPs, $Fe_3O_4$ NPs,and $Fe_3O_4$@ ZnO NCs was carried out on both Gram-positive and Gram-negative bacteria strains. The Gram-positive bacteria Staphylococcus aureus, and Streptococcus pyogen, and the Gram-negative bacteria strains Escherichia-Coli, and Pseudomonas aeruginosa, bacteria were used for antibacterial study. They were obtained from applied biological department laboratory, at Adama Science and Technology University. The bacteria were incubated using nutrient agar and carried out using disc diffusion methods.

## 3.7. Media Preparation and Bacterial Culture

Nutrient agar media were prepared by dissolving of 1.5 g nutrient agar within 100 mL distilled water and then sterilized using autoclave at 120°C for 20 min. After cooling, about 20 mL of medium are added to sterilized Petri dishes. Bacterial cultures were maintained on nutrient agar at 37°C. Four bacterial strains were mixing in nutrient broth and shaken gently at 160rpm to allow equal mixing of bacteria cells with agar and growth for 24hr at 37°C (Akpomie et al., 2021).

## 3.8. Disc Diffusion Method

Antibacterial activity of biosynthesized ZnO NPs, NPs $Fe_3O_4$ and $Fe_3O_4$@ ZnO NCs on Gram-positive (Staphylococcus aureus and Streptococcus pyogen) and Gram-negative (Escherichia coli and P. aeruginosa) bacteria were tested by the disc diffusion method based on the procedures reported (Abbasi et al., 2021). Bacterial suspension was prepared until the concentrations of bacterial suspensions were achieved to 1×108 colony forming units (CFU) $mL^{-1}$ by comparison with 0.5

McFarland standards. Different concentration such as 100, 50g, 25g and 12.5g of each prepared samples were dissolved in 1 mL dimethyl sulfoxide (DMSO) in a test tube as the negative control (NC). The standardized culture of test bacteria was first evenly spread onto the surface of the nutrient agar plates using sterile cotton swabs. 6 mm diameter of filter paper was prepared and placed in different areas of the disc. The soaked dried disks were placed on the Mueller-Hinton agar plates and incubated at 37°C for 24 hours in an incubator. The analysis was conducted in triplicate. A ciprofloxacin 30 µg/mL disk was used as the positive control. Finally, antibacterial activity was then evaluated by measuring the diameter (mm) of the inhibition zone (IZ) around the disc against positive control and each bacteria strain were measured using a ruler and compared results (Gurunathan et al., 2009).

# 4. RESULTS AND DISCUSSIONS

## 4.1 UV–Vis Diffuse Reflectance Spectroscopy (DRS) Analysis

The optical properties and band gap energies of the synthesized ZnO NPs, $Fe_3O_4$ NPs, and $Fe_3O_4$@ZnO nanocomposite were investigated using UV–Vis diffuse reflectance spectroscopy (DRS), as depicted in Figure 7a-c. The reflectance spectra were transformed using the Kubelka–Munk function, $(R) = \frac{(1-R)\text{^}2}{2R}$ , which is proportional to the absorption coefficient for highly scattering samples. The optical band gaps ($E_g$) were determined by extrapolating the linear region of the Tauc plots for direct allowed transitions, plotted as [F(R)hv] ^2 versus photon energy (hv). As shown in the Figure. 7(a), ZnO nanoparticles exhibited a sharp absorption edge around 380 nm, consistent with intrinsic band-to-band transitions. The estimated band gap energy from the Tauc plot (inset) was approximately 2.1 eV. This value is red-shifted compared to bulk ZnO (~3.2 eV), which may be attributed to surface defects, oxygen vacancies, or size-induced quantum confinement effects typically observed in nanoscale materials.

In contrast, $Fe_3O_4$ nanoparticles displayed broader absorption in the visible region, as seen in the Figure. 7(b), likely due to electronic transitions involving $Fe^{2+}/Fe^{3+}$ ions and interband transitions. The calculated band gap energy was 2.0 eV, in good agreement with previously reported values for magnetite nanoparticles (Yetim, 27 August 2020) .This confirms the semiconductor nature of $Fe_3O_4$ with potential light absorption in the visible region.

The DRS spectrum of the $Fe_3O_4$@ZnO nanocomposite is presented in Figure 7(c), exhibiting enhanced absorption across a wider wavelength range. The corresponding Tauc plot revealed band gap energy of 2.3 eV, which is slightly higher than that of the individual ZnO and $Fe_3O_4$ nanoparticles. This band gap widening could be ascribed to interfacial electronic interactions at the $Fe_3O_4$/ZnO heterojunction, as well as possible structural strain or defect modulation introduced during composite formation. The observed shift further supports the formation of a new optical system with synergistically tuned properties.

Generally, the UV–Vis DRS results indicate successful heterostructure formation in the $Fe_3O_4$/@ZnO composite, accompanied by band gap modulation and enhanced optical absorption. These features suggest improved light-harvesting capability,

making the composite a promising candidate for antibacterial, photocatalytic, and optoelectronic applications.

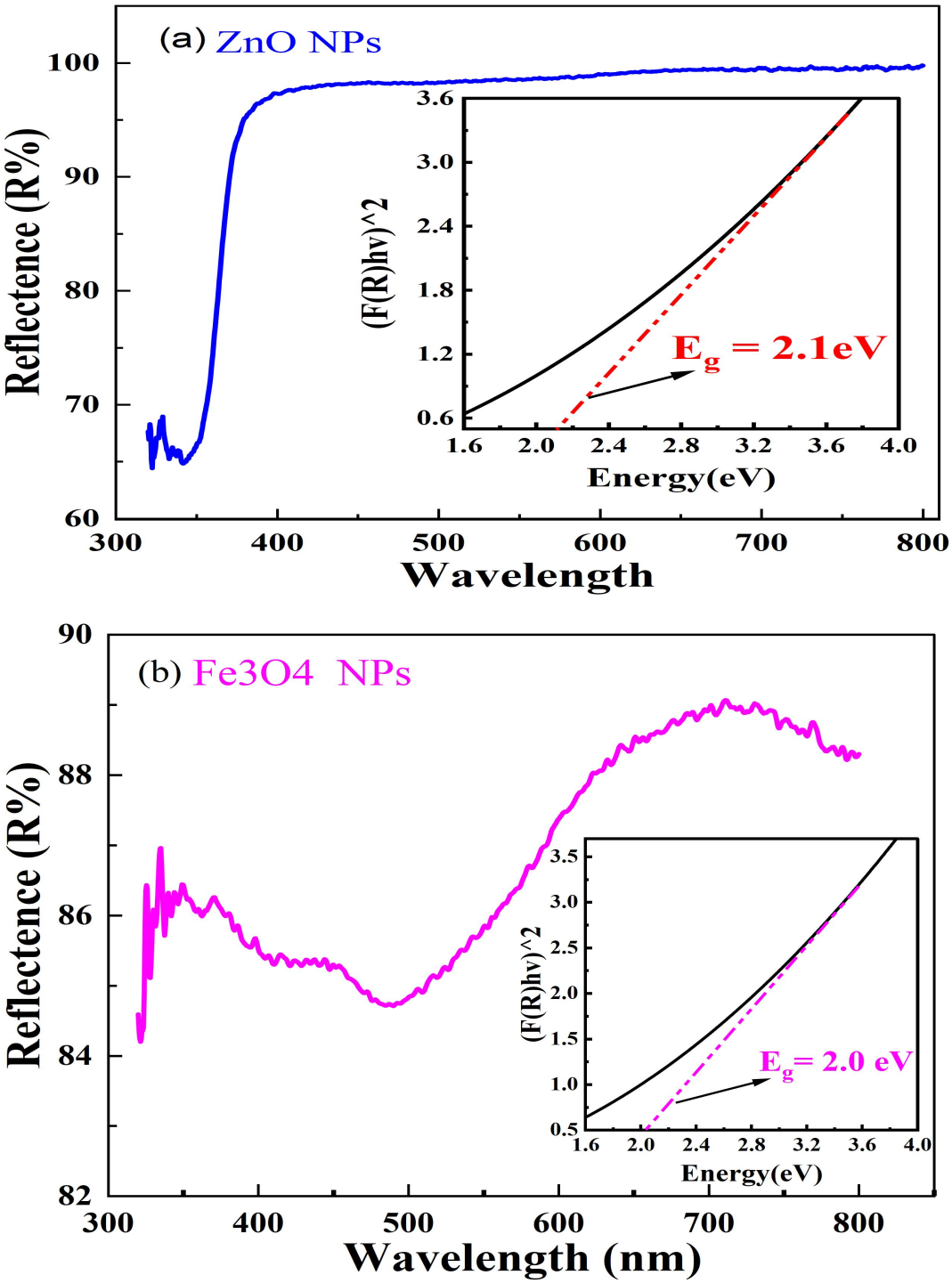

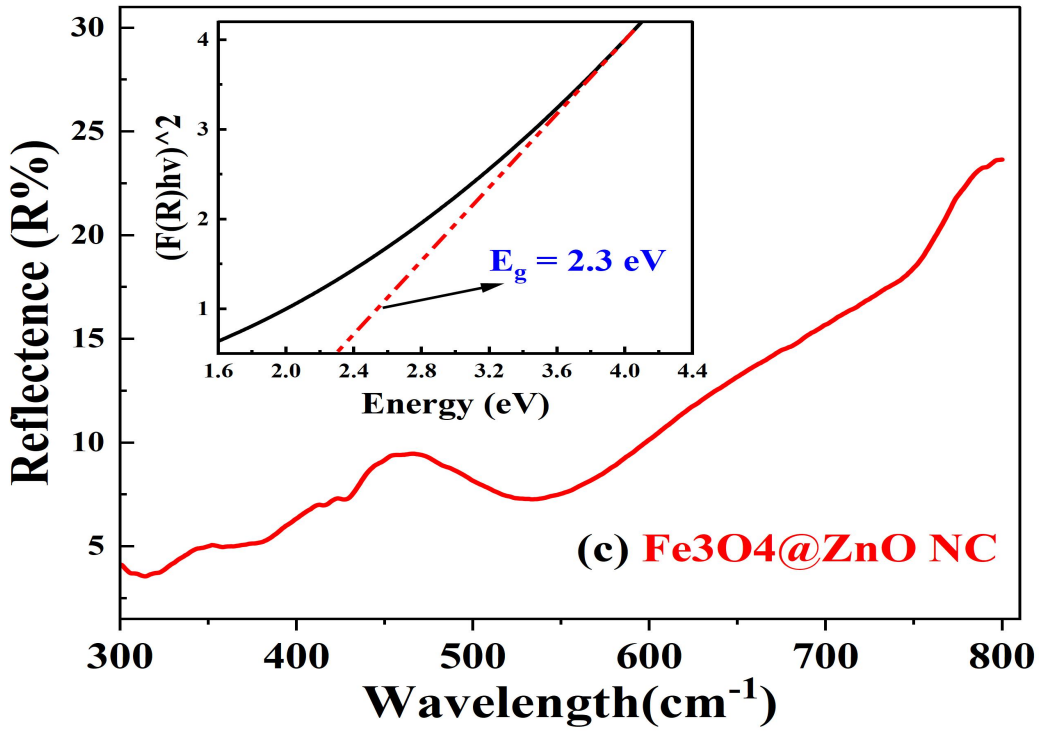


Figure 6. UV–Vis diffuse reflectance spectra (DRS) and Tauc plots of **(a)** ZnO NPs, **(b)** $Fe_3O_4$ NPs, and **(c)** $Fe_3O_4$@ZnO nanocomposite, their optical absorption and band gap energies.

## 4.2 X-ray Diffraction (XRD) Analysis

X-ray diffraction (XRD) is a powerful technique used for both qualitative and quantitative characterization of nanoparticles, particularly for identifying crystal structures and confirming phase formation (Yousaf, 2020) . In this study, XRD analyses were performed to investigate the crystalline structure and phase composition of the synthesized ZnO nanoparticles (ZnO NPs), $Fe_3O_4$ nanoparticles ($Fe_3O_4$ NPs), and the $Fe_3O_4$@ZnO nanocomposite. As shown in the Figure 7, the XRD pattern of ZnO NPs (Figure 7a) exhibits sharp diffraction peaks at 2θ values of 31.73°, 34.37°, 36.21°, 47.51°, 56.55°, 62.79°, and 67.91°, which correspond to the (100), (002), (101), (102), (110), (103), and (112) crystal planes, respectively. These peaks are consistent with the hexagonal wurtzite structure of ZnO (JCPDS card no. 36-1451), indicating high crystallinity and phase purity.

The XRD pattern of $Fe_3O_4$ NPs (Figure 7b) reveals characteristic peaks at 31.80°, 35.63°, 45.55°, 56.56°, and 62.96°, which are indexed to the (220), (311), (400), (422), (511), and (440) planes of the inverse spinel structure of $Fe_3O_4$, matching standard data (JCPDS card no. 19-0629), confirming the successful synthesis of the magnetite

phase with good crystallinity. The $Fe_3O_4$@ZnO NC (Figure 7c) displays a combination of peaks from both ZnO and $Fe_3O_4$, indicating the coexistence of both crystalline phases within the composite structure. No additional peaks related to impurities or secondary phases were observed, suggesting that the integration of ZnO onto $Fe_3O_4$ occurred without altering the structural integrity of the individual components. The (311) peak of $Fe_3O_4$ and the (100) peak of ZnO are especially prominent, suggesting both phases are well retained in the nanocomposite. Slight peak shifts or broadening may indicate interfacial interactions or particle size reduction. These results confirm the successful formation of a well-defined $Fe_3O_4$@ZnO nanocomposite with preserved crystallinity and phase purity.

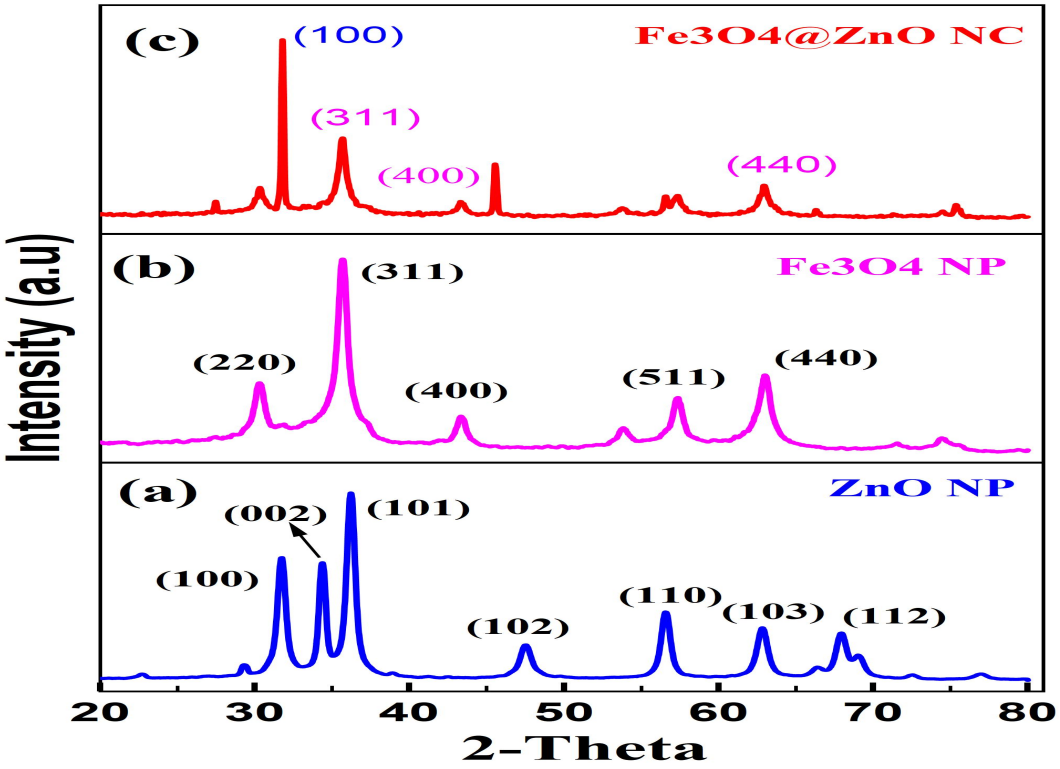


Figure 7. XRD patterns of ZnO NPs (a), $Fe_3O_4$ NPs (b), and $Fe_3O_4$@ZnO nanocomposite (c)

Furthermore, the crystal size of the synthesized material was assessed using Scherrer's equation (Eq. 1).

$$D = \frac{K\lambda}{\beta \cos\theta} \qquad 1$$

where D is the size of the crystal, λ is the X-ray wavelength, β is the full width at half maximum intensity of the peak [rad], and θ is the Bragg's angle of diffraction. Using Eq. (1), the average crystal size of ZnO NPs was estimated to be 16.3 nm, indicating

the formation of nanosized particles with relatively high crystallinity. However, $Fe_3O_4$ has a larger crystal size of 42.0 nm, suggesting extensive crystal growth during synthesis. The $Fe_3O_4$@ZnO nanocomposite has a smaller size of 14.9 nm, slightly lower than that of ZnO NPs. This reduction may be attributed to structural strain or mutual inhibition of crystal growth resulting from the interaction between the $Fe_3O_4$ and ZnO phases. The decrease in crystallite size is expected to enhance the material's functional properties, such as antibacterial activity, photocatalysis, and magnetic separation.

Table 2. XRD data of synthesized ZnO NPs, $Fe_3O_4$ NPs, and $Fe_3O_4$/ZnO NCs

| Sample Name | 2θ (°) | FWHM (°) | FWHM (rad) | θ (°) | cos θ | D (nm) | Average D (nm) |
|---|---|---|---|---|---|---|---|
| ZnO NPs | 31.73 | 0.51950 | 0.00907 | 15.86 | 0.961 | 17.0 | 16.3 |
| | 34.37 | 0.40560 | 0.00708 | 17.18 | 0.955 | 22.6 | |
| | 36.21 | 0.53670 | 0.00937 | 18.10 | 0.950 | 16.3 | |
| | 47.51 | 0.73140 | 0.01277 | 23.75 | 0.915 | 12.4 | |
| | 56.55 | 0.56680 | 0.00989 | 28.27 | 0.881 | 16.5 | |
| | 62.79 | 0.66100 | 0.01154 | 31.39 | 0.853 | 14.7 | |
| | 67.91 | 0.68670 | 0.01199 | 33.95 | 0.829 | 14.9 | |
| $Fe_3O_4$ NPs | 31.80 | 0.15610 | 0.00272 | 15.90 | 0.961 | 55.3 | 42.0 |
| | 35.63 | 0.44800 | 0.00782 | 17.81 | 0.952 | 20.1 | |
| | 45.55 | 0.16870 | 0.00294 | 22.77 | 0.922 | 53.4 | |
| | 56.56 | 0.20570 | 0.00359 | 28.28 | 0.881 | 45.8 | |
| | 62.96 | 0.27330 | 0.00477 | 31.48 | 0.853 | 35.6 | |
| $Fe_3O_4$@ZnO NC | 30.31 | 0.59000 | 0.01030 | 15.15 | 0.965 | 15.8 | 14.9 |
| | 35.67 | 0.64000 | 0.01117 | 17.83 | 0.952 | 13.7 | |
| | 43.33 | 0.57500 | 0.01004 | 21.66 | 0.929 | 15.5 | |
| | 57.33 | 0.63000 | 0.01100 | 28.66 | 0.877 | 15.1 | |
| | 62.95 | 0.65000 | 0.01134 | 31.47 | 0.853 | 14.2 | |

## 4.1. Fourier Transform Infrared Spectroscopy (FTIR) Analysis

Fourier transform infrared (FTIR) spectroscopy is a valuable tool for identifying functional groups and biomolecules involved in the reduction, stabilization, and capping of synthesized nanoparticles (NPs) and nanocomposites (NCs) (Zuk, 2025). In this study, FTIR analysis was conducted to investigate the chemical interactions and functional groups present in the *Vernonia amygdalina* leaf extract, zinc oxide

nanoparticles (ZnO NPs), iron oxide nanoparticles ($Fe_3O_4$ NPs), and their hybrid $Fe_3O_4$@ZnO nanocomposite (NC). The FTIR spectra, recorded in the range of 400–4000 cm-$^1$, are presented in Figure 9 and provide valuable insights into the molecular composition and bonding characteristics of a sample.

The FTIR spectrum of the plant extract (Figure 9a) exhibited prominent absorption bands indicative of organic biomolecules. A broadband at 3284 cm$^{-1}$ corresponds to O–H stretching vibrations, typically arising from phenolic compounds, polysaccharides, or adsorbed water. The sharp peak at 2919 cm$^{-1}$ is attributed to C–H stretching in aliphatic hydrocarbons. A strong band at 1738 cm$^{-1}$ corresponds to C=O stretching vibrations from ester groups. Additional peaks at 1593 cm$^{-1}$ (aromatic C=C or N–H bending), 1373 cm$^{-1}$ (C–H bending), and 1046 cm$^{-1}$ (C–O stretching in carbohydrates) confirm the presence of lignin, proteins, and cellulose. A minor peak at 522 cm$^{-1}$ may be attributed to inorganic mineral residues. The FTIR spectrum of ZnO NPs in (Figure 9b) shows a strong Zn–O phonon mode at 421 cm$^{-1}$, confirming the formation of the ZnO crystalline phase. A broad absorption band at 3369 cm$^{-1}$ corresponds to O–H stretching of surface-adsorbed water, while peaks at 1728 cm$^{-1}$ (C=O) and 1361 cm$^{-1}$ (Zn–O–H bending) indicate slight organic residues from the synthesis process. Complementarily, $Fe_3O_4$ NPs (Figure 9c) displayed a prominent Fe–O stretching vibration at 435 cm$^{-1}$, characteristic of the spinel structure of magnetite. Weak bands at 3264 cm$^{-1}$ (O–H stretching) and 1591 cm$^{-1}$ (residual organics) suggest the presence of organic molecules, possibly from the plant extract, acting as stabilizing agents.

Importantly, the FTIR spectrum of the $Fe_3O_4$@ZnO nanocomposite (Figure 9d) reveals a shifted Fe–O/Zn–O vibrational band at 448 cm$^{-1}$, which lies intermediate between those of $Fe_3O_4$ and ZnO, indicating successful nanocomposite formation and possible chemical interaction at the oxide interfaces. The continued presence of organic-related peaks, such as C–O stretching at 1120 cm$^{-1}$ and the merged band at 1374 cm$^{-1}$, suggests overlapping vibrational modes from ZnO and $Fe_3O_4$ nanoparticles. These features also point to the presence of residual surfactants or phytochemicals. Overall, FTIR analysis confirmed that phytochemicals present in *Vernonia amygdalina* leaf extract played a significant role as reducing, capping, and stabilizing agents during nanoparticle synthesis. Their presence helped prevent aggregation and contributed to the successful formation of a stable $Fe_3O_4$@ZnO nanocomposite

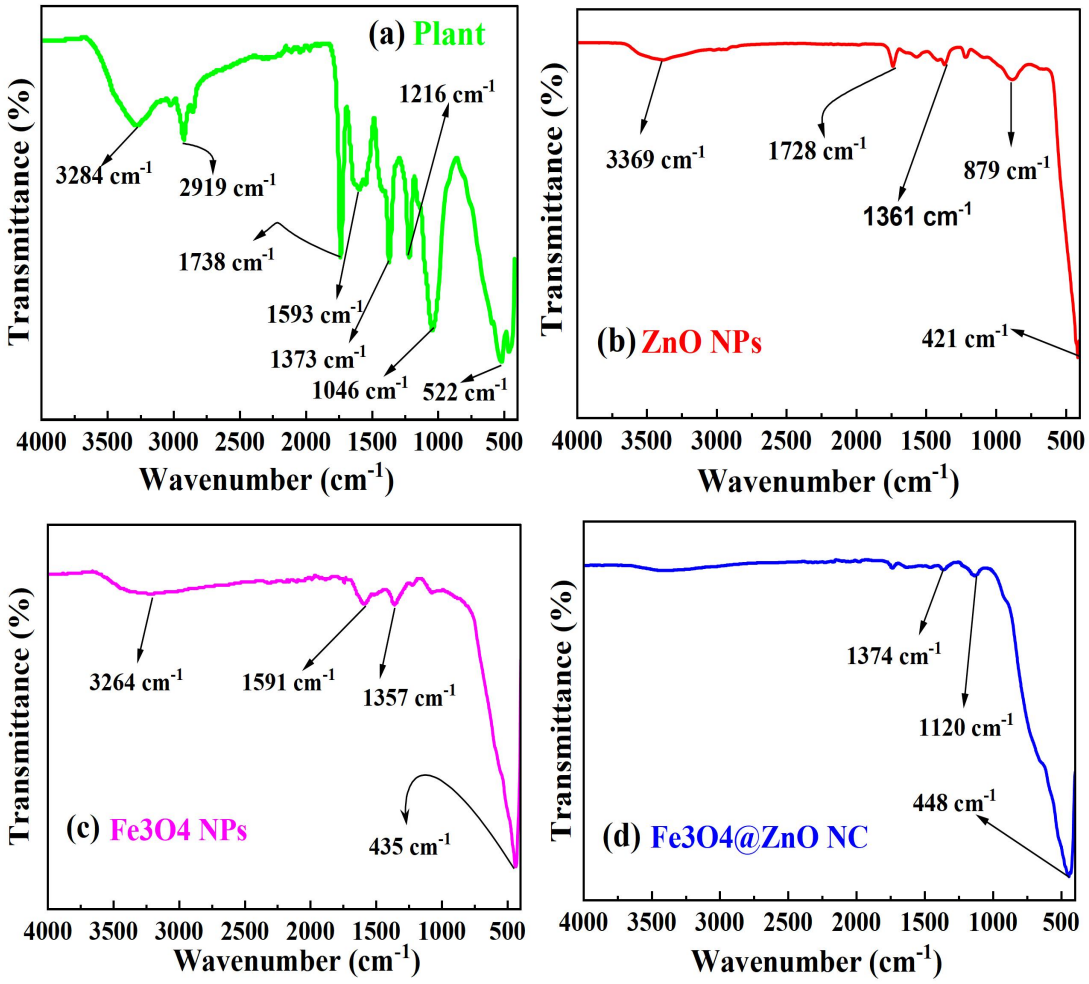


Figure 8. FTIR Spectra of **(a)** *Vernonia amygdalina* Leaf Extract, **(b)** ZnO Nanoparticles,**(c)** $Fe_3O_4$ Nanoparticles, and **(d)** $Fe_3O_4$@ZnO Nanocomposite.

## 4.4. Scanning Electron Microscopy (SEM) Analysis

From known analytical techniques electron microscopy techniques, SEM is one microscopic technique and can govern the surface morphology of nanoparticles and nanocomposites, such as their shape, size, and particle size distribution, which was evaluated through histogram analysis (Machovsky et al., 2012). The findings of the SEM and histogram analysis are accessible in Figure 10 below. These investigate insights into the physical characteristics and structural integrity of ZnO NPs, $Fe_3O_4$ NPs, and $Fe_3O_4$@ZnO nanocomposites. As shown in Figure 10(a), the ZnO nanoparticles display a dense and compact granular texture, with significant surface heterogeneity, which may enhance contact with bacterial cells and improve antibacterial efficiency. In Figure 10(b), the results reveal that the $Fe_3O_4$ nanoparticles have a moderately aggregated morphology, with irregular yet predominantly spherical

particles, likely due to strong magnetic interactions. This porous structure could enhance surface area and make $Fe_3O_4$ more reactive. As illustrated in Figure 10(c), the $Fe_3O_4$@ZnO nanocomposite exhibits a more complex and heterogeneous morphology, characterized by the uniform dispersion of finely distributed ZnO and $Fe_3O_4$ nanoparticles across its surface. Fibrous and flake-like structures, possibly originating from organic residues or strong interaction zones between the two nanoparticle types, are visible. This structural integration suggests the successful formation of the nanocomposite and highlights the potential for synergistic antibacterial activity.

The particle size distribution of the $Fe_3O_4$@ZnO nanocomposite in Figure 10(d) is narrow and uniform, with an average particle size of approximately 20 nm, and the particle size distribution was calculated from a histogram, considering 200 particles, from which the average $Fe_3O_4$@ZnO nanocomposite size was measured using ImageJ software. This nanoscale range is favorable for biological applications, as smaller particles offer a higher surface area-to-volume ratio, enhancing interaction with microbial membranes and contributing to effective antibacterial mechanisms. The $Fe_3O_4$@ZnO nanocomposite demonstrates an integrated structure and optimal size distribution, suggesting its potential as an efficient multifunctional agent in antibacterial applications.

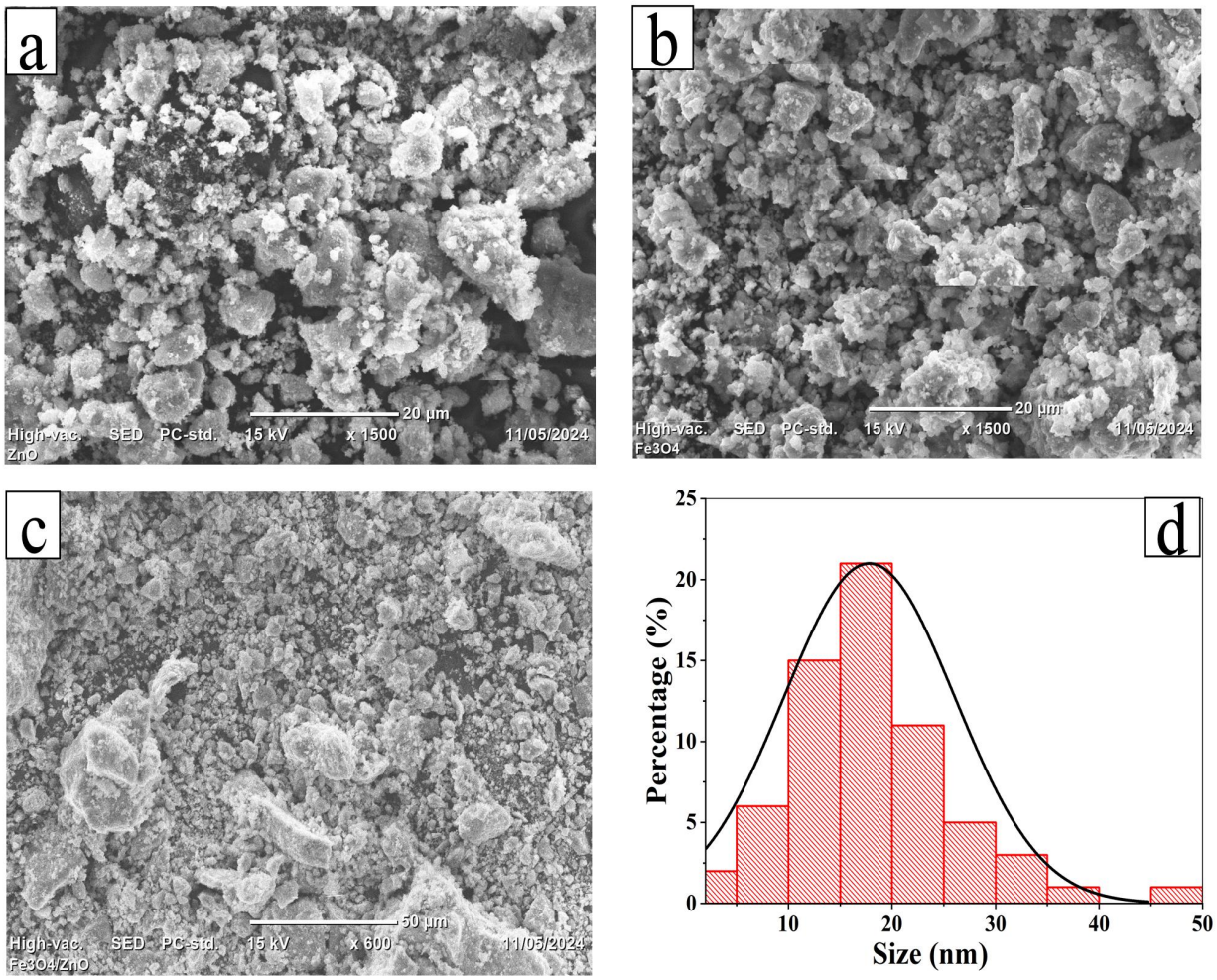


Figure 9.**(a-c)** SEM micrographs of ZnO NPs, $Fe_3O_4$ NPs, and $Fe_3O_4$/ZnO nanocom posite, and **(d)** particle size distribution histograms of $Fe_3O_4$/ZnO nanocomposite

### 4.5.1. Antibacterial Activity of ZnO NPs, $Fe_3O_4$NPs, and $Fe_3O_4$@ZnO Ncs

The appearance of metal oxide nanoparticles has transformed antibacterial applications through their unique physicochemical properties and mechanisms of action. Recent research establishes that zinc oxide nanoparticles (ZnO NPs), iron oxide nanoparticles ($Fe_3O_4$ NPs), and $Fe_3O_4$@ZnO nanocomposites display significant antibacterial activities against a broad spectrum of pathogens. These nanomaterials display improved capability because of their size-dependent action, high surface responsiveness, and synergistic belongings when combined into composite structures. This finding surveys the antibacterial properties, mechanisms of action, and potential applications of these nanomaterials as promising antimicrobial agents.

### 4.5.2. Properties and Antibacterial Mechanisms of ZnO Nanoparticles

Zinc oxide nanoparticles have gained considerable attention for their remarkable antibacterial properties, primarily attributed to their increased specific surface area and enhanced particle surface reactivity at nanoscale dimensions. ZnO NPs are recognized as a bio-safe material with significant photo-oxidizing and photocatalytic capabilities affecting both chemical and biological species. In their nanoform, ZnO particles can adopt various morphologies, including rod-shaped structures with aspect ratios of approximately 3, which significantly influence their interaction with bacterial cells. The antibacterial efficacy of ZnO NPs is strongly dependent on their physical properties. Particle size plays a crucial role, with smaller nanoparticles demonstrating enhanced antibacterial activity. Research has shown that ZnO nanorods with diameters smaller than 50 nm exhibit superior antibacterial performance compared to those with larger dimension (Parveen et al., 2016). This size-dependent activity can be attributed to the increased surface-to-volume ratio that facilitates greater interaction with bacterial cell surfaces and potentially improves cellular penetration.

### 4.5.3. Mechanisms of Antibacterial Action

The bactericidal and bacteriostatic effects of ZnO NPs involve multiple mechanisms. Primarily known pathway is the generation of responsive oxygen species (ROS), including hydroxyl radicals ($OH^-$), hydrogen peroxide ($H_2O_2$), and peroxide ($O_2^{-2}$). These highly responsive species cause oxidative stress to bacterial cells, leading to a cascade of detrimental effects. The generation of ROS subsidizes to cell wall damage through limited to a small area interactions with ZnO particles, enhanced membrane permeability, and internalization of nanoparticles due to disruption of the proton motive force. The release of zinc ions ($Zn^{2+}$) represents another important antibacterial mechanism. As ZnO NPs dissolve in aqueous environments, they release $Zn^{2+}$ ions that can be taken up by bacterial cells, disrupting essential cellular functions. This combined effect of ROS generation and zinc ion release leads to mitochondrial weakness, intracellular content leakage, and altered gene expression related to oxidative stress, ultimately resulting in cell growth inhibition (N. Ali et al., 2024).

### 4.5.4. Antibacterial Properties of $Fe_3O_4$ Nanoparticles

Iron oxide nanoparticles form in inverse spinel structures and typically exhibit well-dispersed spherical morphologies. These nanoparticles possess magnetic properties that can be advantageous for certain applications, allowing for their manipulation and

recovery using external magnetic fields. The small size and high surface area of $Fe_3O_4$ NPs contribute to their reactivity and interaction with bacterial cells.

### 4.5.5. Mechanisms of Antibacterial Action

Iron oxide nanoparticles display antibacterial activity primarily through the generation of responsive oxygen species on their surfaces. The production of ROS leads to oxidative stress in bacterial cells, destructive essential cellular components such as membranes, proteins, and DNA. Although the ROS-generating capability of $Fe_3O_4$ NPs might be less potent than that of ZnO NPs, the particles still demonstrate significant antibacterial effects, particularly against common pathogens like *E. coli and S. aureus* (Soliman & Moustafa, 2020). The magnetic properties of $Fe_3O_4$ NPs also offer additional benefits for antibacterial applications. These properties can facilitate the aggregation of bacteria through magnetic attraction, potentially enhancing the contact between the nanoparticles and bacterial cells, thereby improving antibacterial efficacy.

### 4.5.6. Antibacterial Activity of $Fe_3O_4$@ ZnO Nanocomposites

The combination of $Fe_3O_4$ and ZnO into nanocomposites represents a strategic way to improve antibacterial activity through synergistic effects. $Fe_3O_4$/ZnO composites maintain a homogeneous distribution of both phases and demonstrate excellent colloidal stability in aqueous environments. This stability is crucial for maintaining consistent antibacterial activity in various applications. While ZnO provides strong photocatalytic activity and ROS generation capabilities, $Fe_3O_4$ adds magnetic properties and additional pathways for ROS production. The structural integration of these components creates a multifunctional material with improved antibacterial characteristics.

The antibacterial activity of $Fe_3O_4$/ZnO nanocomposites is significantly improved compared to the individual components due to more than a few synergistic mechanisms. First, the combination of ROS generation from both ZnO and $Fe_3O_4$ surfaces leads to increased oxidative stress on bacterial cells.

Second, the composite structure can potentially reduce electron/hole recombination rates, thereby improving the efficiency of ROS production. The magnetic properties contributed by the $Fe_3O_4$ component provide additional advantages, such as dispersion and stability of the nanocomposite. These properties can also facilitate the

recovery and reuse of the material in various applications, enhancing its practical utility as an antibacterial agent (Hasan, 2015).

### 4.5.7. Disk Diffusion Methods

Clinical bacterial strains from the American Type Culture Collection (ATCC), including *Escherichia coli* (ATCC 25922), *Pseudomonas aeruginosa* (ATCC 27853), *Streptococcus pyogenes* (ATCC 19615), and *Staphylococcus aureus* (ATCC 25923), were used to evaluate the antibacterial activity of different nanoparticle (NP) formulations. These standard bacterial cultures were obtained from the Ethiopian Biodiversity Institute in Addis Ababa. To standardize bacterial density, a 0.5 McFarland standard was prepared by mixing 99.95 mL of 1% $H_2SO_4$ with 0.05 mL of 1% $BaCl_2$ in distilled water. The resulting turbidity was verified using a UV-Vis spectrophotometer at 600 nm, with an absorbance reading of 0.11.

The antibacterial activity of the synthesized nanoparticles was assessed using the disk diffusion method. Nanoparticles were dissolved in dimethyl sulfoxide (DMSO) to prepare concentrations of 100, 50, 25, and 12.5 mg/mL. Bacterial suspensions were adjusted to match the 0.5 McFarland standard, corresponding to approximately $1.5 \times 10^8$ CFU/mL.

Each suspension was uniformly inoculated onto Mueller-Hinton agar plates using a sterile cotton swab. The plates were then allowed to dry for 15 minutes inside a biological safety cabinet. Sterile paper disks were soaked in the prepared NP solutions at varying concentrations and allowed to dry before being placed on the inoculated agar plates. Plates were incubated at 37°C for 24 hours. All tests were conducted in triplicate. A 30 µg/mL ciprofloxacin disk served as a positive control.

Following incubation, the diameters of the inhibition zones were measured in millimeters using a digital antibiotic zone reader. As illustrated in Figure 11 (a, b, c), which presents the antibacterial performance of various materials, the test organisms (*E. coli*, *P. aeruginosa*, *S. aureus*, and *S. pyogenes*) showed different levels of sensitivity to the nanoparticle formulations. The filter paper disks treated with 12.5 mg/mL NPs or NCs showed less prominent inhibition zones, indicating limited antibacterial activity at this lower dose. However, as the concentration increased, so

did the size of the inhibition zones, reflecting a dose-dependent antibacterial effect (Taha Yassin et al., 2024).

Moreover, at identical concentrations, nanocomposites (NCs) exhibited larger zones of inhibition compared to the individual nanoparticles (NPs), suggesting enhanced antibacterial efficacy of the composite materials. These findings indicate that NCs are more effective than NPs alone, aligning with or exceeding results reported in previous studies (Khairy et al., 2024) .

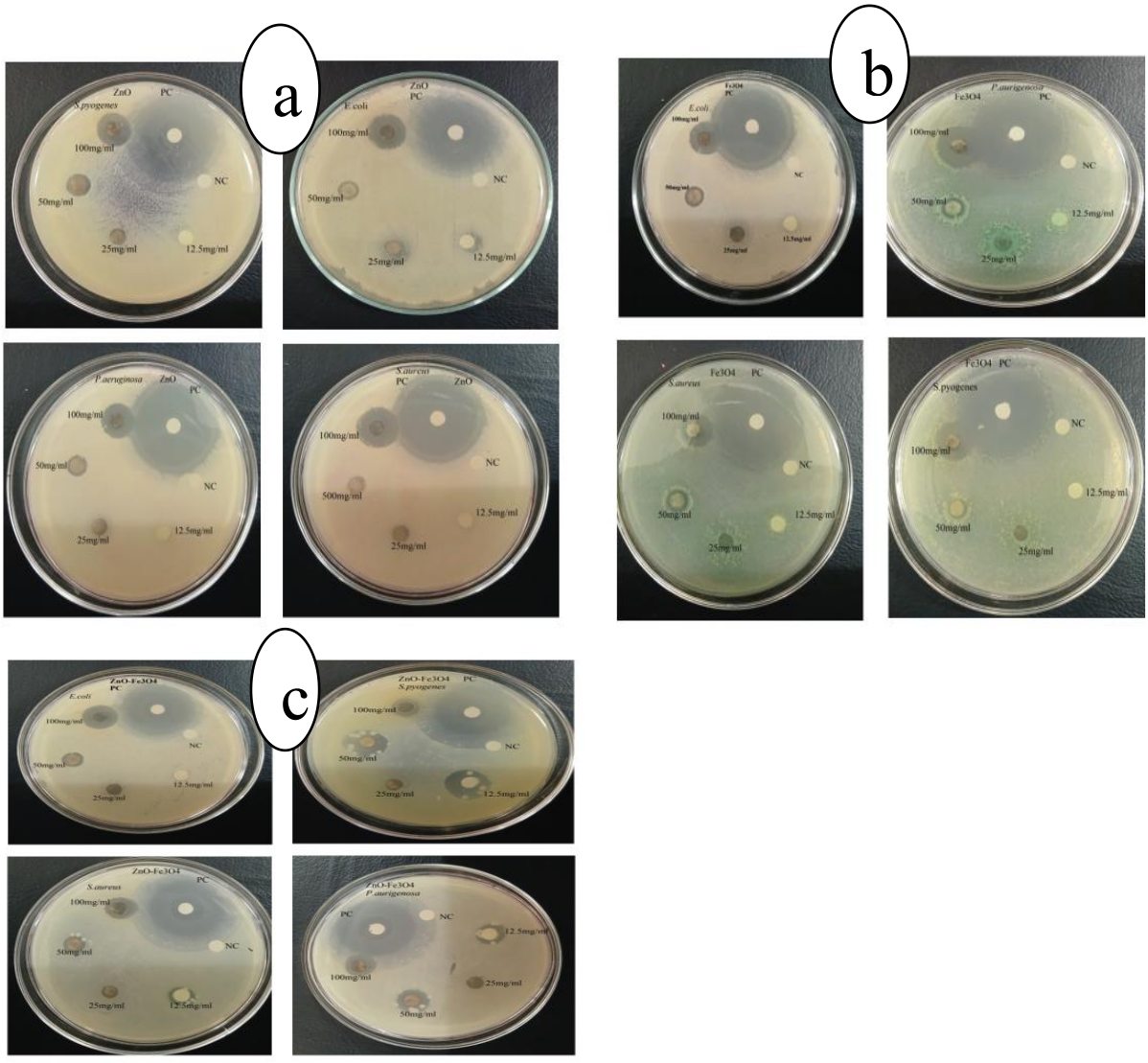


Figure 10. Photographs of antibacterial activities of **(a)** ZnO NPs,**(b)** $Fe_3O_4$ NPs, **(c)** ZnO-$Fe_3O_4$ NCs.

Table 3. Antibacterial Activity of ZnO NPs, $Fe_3O_4$ NPs, and $Fe_3O_4$@ ZnO Nanocom posite: Inhibition zone diameters (mm) at different concentrations

| **NPs/NCs and Organisms** | | | **Dilution Results, Means of three replications, and Standard error (±SE) of Inhibition zones in mm** | | | | | |
|---|---|---|---|---|---|---|---|---|
| S/N | NP/NC | Types of Organisms | 100 mg/mL | 50 mg/mL | 25 mg/mL | 12.5 mg/mL | PC (+ve) | NC (-ve) |
| 1 | ZnO NPs | E. coli | 9.6 | 8.3 | 6.6 | 6.5 | 24.6 | 6 |
| | | P. aeruginosa | 10.3 | 9 | 8.5 | 7.6 | 22.6 | 6 |
| | | S. aureus | 9.3 | 8.6 | 7.6 | 6.6 | 23.6 | 6 |
| | | S. pyogenes | 10.6 | 9.3 | 8.6 | 6.3 | 23.6 | 6 |
| 2 | $Fe_3O_4$ NPs | E. coli | 9 | 7.6 | 7.6 | 6.6 | 24 | 6 |
| | | P. aeruginosa | 8 | 7.7 | 6.5 | 6.3 | 21.3 | 6 |
| | | S. aureus | 9.3 | 8.6 | 8.5 | 7.6 | 22.6 | 6 |
| | | S. pyogenes | 10 | 9 | 8.3 | 6.6 | 23.6 | 6 |
| 3 | $Fe_3O_4$@ ZnO NC | E. coli | 10 | 9 | 8.3 | 6.5 | 23.6 | 6 |
| | | P. aeruginosa | 10.3 | 9.3 | 6.6 | 6.3 | 24 | 6 |
| | | S. aureus | 11 | 10 | 8.6 | 6.5 | 23.6 | 6 |
| | | S. pyogenes | 12 | 10.6 | 9.3 | 8.3 | 24 | 6 |

As illustrated in the above table, the findings confirms that the antibacterial activities of ZnO nanoparticles (ZnO NPs), $Fe_3O_4$ nanoparticles ($Fe_3O_4$ NPs), and the $Fe_3O_4$@ZnO nanocomposite (NC) were evaluated using the disk diffusion method against four bacterial strains: *Escherichia coli*, *Pseudomonas aeruginosa*, *Staphylococcus aureus*, and *Streptococcus pyogenes*. The synthesized applicants were tested at concentrations of 100, 50, 25, and 12.5 mg/mL. The findings publicized that ZnO NPs displayed superior antibacterial activity than $Fe_3O_4$ NPs in most cases. At the maximum concentration (100 mg/mL), ZnO NPs showed inhibition zones of 9.6 mm, 10.3 mm, and 10.6 mm against *E. coli*, *P. aeruginosa*, and *S. pyogenes*, respectively, compared to 9.0 mm, 8.0 mm, and 10.0 mm for $Fe_3O_4$ NPs. Both nanoparticles had the same inhibition zone (9.3 mm) against *S. aureus* at this concentration. The superior performance of ZnO NPs may be attributed to their ability to generate reactive oxygen species (ROS), release $Zn^{2+}$ ions, and interact with bacterial cell membranes, leading to cell wall damage and metabolic disruption. In

contrast, $Fe_3O_4$ NPs showed moderate antibacterial activity, with slightly higher inhibition against *S. aureus* at lower concentrations, possibly due to iron-mediated oxidative stress or strain-specific sensitivity.

The $Fe_3O_4$@ZnO nanocomposite presented significantly improved antibacterial activity compared to the individual nanoparticles. At 100 mg/mL, the nanocomposite produced the largest inhibition zones: 10.0 mm (*E. coli*), 10.3 mm (*P. aeruginosa*), 11.0 mm (*S. aureus*), and 12.0 mm (*S. pyogenes*). These values were consistently higher across all tested concentrations. The better-quality performance of the nanocomposite may be due to the combined antimicrobial mechanisms of both components, including dual ion release ($Zn^{2+}$ and $Fe^{2+}/Fe^{3+}$), enhanced ROS production, and augmented surface area, prominent to better interaction with bacterial cells. The positive control (a standard antibiotic) produced the largest inhibition zones (21.3–24.6 mm), confirming the sensitivity of the test organisms, while the negative control (likely sterile water or solvent) showed no inhibition, validating the antimicrobial activity of the synthesized nanomaterials. Generally, the findings obtained from the disk diffusion assay showed that $Fe_3O_4$@ZnO nanocomposite exhibited the strongest antibacterial potential and may serve as a auspicious applicant for future antimicrobial applications.

# 5. CONCLUSION and RECOMMENDATION

## 5.1. Conclusion

The $Fe_3O_4$@ZnO nanocomposite was successfully synthesized using a cost-effective, non-toxic, and environmentally friendly aqueous method at room temperature, without the need for sophisticated equipment. The surface modification of magnetite enabled effective deposition of ZnO, creating structural mismatches that introduced more photocarrier traps and reduced radiative recombination-factors beneficial for enhancing antibacterial activity. This study confirmed the effective synthesis and inclusive characterization of ZnO nanoparticles, $Fe_3O_4$ nanoparticles, and their $Fe_3O_4$@ZnO nanocomposite using frequent analytical techniques. The results revealed better-quality optical properties, well-defined crystalline structures, and a characteristic morphology for the nanocomposite. The use of *Vernonia amygdalina* leaf extract played a vital role in the biogenic synthesis, serving as both a reducing and stabilizing agent. Prominently, the $Fe_3O_4$@ZnO nanocomposite showed meaningfully improved antibacterial activity compared to the individual nanoparticles, emphasizing its potential as auspicious applicant for future antibacterial applications.

## 5.2. Recommendation

As a future prospective, to enhance the antibacterial effectiveness of biologically synthesized $Fe_3O_4$@ZnO nanocomposites, different synthesis strategies such as core-shell structures, doping, and surface coating methods should be explored. The antibacterial activity may also be improved under UV light exposure, which can activate photocatalytic properties of the nanocomposite. For practical application, collaboration with healthcare professionals such as doctors, pharmacists, and researchers from medical institutions should be considered to facilitate real-world testing and implementation. Moreover, detailed chemical analysis of the synthesized $Fe_3O_4$@ZnO nanocomposites, including their elemental composition and oxidation states, should be conducted using X-ray Photoelectron Spectroscopy (XPS). In addition to antimicrobial applications, the potential of these nanocomposites as reusable nano-adsorbents for the removal of environmental pollutants, such as hexavalent chromium ($Cr^{6+}$) ions, should be investigated in future study.

# REFERENCES


Agarwal, H., Kumar, S. V., & Rajeshkumar, S. (2017). Resource-Efficient Technologies Review article A review on green synthesis of zinc oxide nanoparticles – An eco-friendly approach. *Resource-Efficient Technologies*, *3*(4), 406–413. https://doi.org/10.1016/j. reffit.2017.03.002

Ahmed, S., Ali, S., & Ikram, S. (2017). Journal of Photochemistry & Photobiology , B : Biology A review on biogenic synthesis of ZnO nanoparticles using plant extracts and microbes : A prospect towards green chemistry. *JPB*, *166*, 272–284. https://doi.org/10.1016/j.j photobiol.2016.12.011

Akpomie, K. G., Ghosh, S., Gryzenhout, M., & Conradie, J. (2021). *Ananas comosus peel – mediated green synthesized magnetite nanoparticles and their antifungal activity against four filamentous fungal strains*.

Al-Rajhi, A. M. H., Abdelghany, T. M., Almuhayawi, M. S., Alruhaili, M. H., Al Jaouni, S. K., & Selim, S. (2024). The green approach of chitosan/Fe2O3/ZnO-nanocomposite synthesis with an evaluation of its biological activities. *Applied Biological Chemistry*, *67*(1). https://doi.org/10.1186/s13765-024-00926-2

Al Rugaie, O., Jabir, M. S., Mohammed, M. K. A., Abbas, R. H., Ahmed, D. S., Sulaiman, G. M., Mohammed, S. A. A., Khan, R. A., Al-Regaiey, K. A., Alsharidah, M., Mohany, K. M., & Mohammed, H. A. (2022). Modification of SWCNTs with hybrid materials ZnO–Ag and ZnO–Au for enhancing bactericidal activity of phagocytic cells against Escherichia coli through NOX2 pathway. *Scientific Reports*, *12*(1), 1–12. https://doi.org/10.1038/s41598-022-22193-1

Ali, N., Younis, M., Ahmed, S., Sara, S., Hanee, U., Ahmed, N., & Durmaz, F. (2024). *Green synthesis of ZnO / Fe 3 O 4 nanoparticles with nigella sativa extract : Efficient degradation of methylene blue and antimicrobial properties*. *43*(4), 116–129.

Ali, U. (2020). *Therapeutic Evaluation of ZnO Nanoparticles Prepared Using Extract of Nigella sativa Seeds*.

Amin, G., Asif, M. H., Zainelabdin, A., Zaman, S., Nur, O., & Willander, M. (2011). *Influence of pH , Precursor Concentration , Growth Time , and Temperature on the Morphology of ZnO Nanostructures Grown by the Hydrothermal Method*. *2011*. https://doi.org/ 10.1155/2011/269692

Anuradha, C. T., & Raji, P. (2021). Citrus limon fruit juice-assisted biomimetic

synthesis, characterization and antimicrobial activity of cobalt oxide (Co3O4) nanoparticles. *Applied Physics A: Materials Science and Processing*, *127*(1), 1–9. https://doi.org /10.1007/s00339-020-04209-7

Atla, S. B., Lin, W., Chien, T., Tseng, M., Shu, J., Chen, C., & Chen, C. (2018). Fabrication of Fe 3 O 4 / ZnO magnetite core shell and its application in photocatalysis using sunlight. *Materials Chemistry and Physics*, *216*(May), 380–386. https://doi.org/10. 1016/j.matchemphys.2018.06.020

Bekele, E. T., Murthy, H. C. A., Muniswamy, D., Lemenh, Y. A., Shume, M. S., Ayanie, G. T., Kumar, A. P., Ravikumar, C. R., Balachandran, R., & Roy, A. (2022). *Solanum tuberosum Leaf Extract Templated Synthesis of Co 3 O 4 Nanoparticles for Electrochemical Sensor and Antibacterial Applications*. *2022*(16 mm).

Chandekar, K. V, Shkir, M., Khan, A., Al-shehri, B. M., & Ghaithan, H. (2020). Journal of Photochemistry & Photobiology A : Chemistry A facile one-pot flash combustion synthesis of La @ ZnO nanoparticles and their characterizations for optoelectronic and photocatalysis applications. *Journal of Photochemistry & Photobiology, A: Chemistry*, *395*(January), 112465. https://doi.or g/10.1016 /j.jphotochem.2020.112465

Drug, D. (2021). *Green Synthesis and Biomedical Applications of ZnO Nanoparticles : Role of PEGylated-ZnO Nanoparticles as*. *231*, 1–19.

Dwivedi, P., Jatrana, I., Khan, A. U., Khan, A. A., Satiya, H., Khan, M., Moon, I. S., & Alam, M. (2021). *Photoremediation of methylene blue by biosynthesized ZnO / $Fe_3O_4$ nano composites using Callistemon viminalis leaves aqueous extract : A comparative study*. 1912–1925.

Frey, A., Lacasella, E. L., Jensen, M. P., & Dutton, P. H. (2025). *Whole mitochondrial DNA sequencing improves resolution of population structure for Paci fi c green turtles ( Chelonia mydas )*. *May*, 1–10. https://doi.org/10. 3389 /fmars.2025.1581306

Geneti, S. T., Mekonnen, G. A., Murthy, H. C. A., Mohammed, E. T., Ravikumar, C. R., Gonfa, B. A., & Sabir, F. K. (2022). *Biogenic Synthesis of Magnetite Nanop articles Using Leaf Extract of Thymus schimperi and Their Application for Monocomponent Removal of Chromium and Mercury Ions from Aqueous Solution*. *2022*(Ii).

Ghaem, E. N., Dorranian, D., & Sari, A. H. (2019). *Characterization of cobalt oxide*

*nanopart icles produced by laser ablation method: effects of laser fluence*. https://doi.org /10.10 16/j.physe.2019.113670

Gul, M., Kashif, M., & Shahid, K. (2024). *Eco-Friendly Approaches in the Synthesis of ZnO Nanoparticles using Plant Extract : A Review*. *3*(July), 1–25.

Gurunathan, S., Kalishwaralal, K., Vaidyanathan, R., Hariharan, N., & Hyun, S. (2009). *Collo ids and Surfaces B : Biointerfaces Biosynthesis , purification and characterization of silver nanoparticles using Escherichia coli*. *74*, 328–335. https://doi. org/10.1016 /j.colsurfb.2009.07.048

Hasan, S. (2015). *A Review on Nanoparticles : Their Synthesis and Types Biosynthesis : Mechanism*. *4*, 9–11.

Iravani, S., & Varma, R. S. (2020). Sustainable synthesis of cobalt and cobalt oxide nanoparticles and their catalytic and biomedical applications. *Green Chemistry*, *22*(9), 2643–2661. https://doi.org/10.1039/d0gc00885k

Khairy, T., Amin, D. H., Salama, H. M., Mohamed, I., Elkholy, A., Elnakib, M., & Gebreel, H. M. (2024). *Antibacterial activity of green synthesized copper oxide nanoparticles against multidrug- resistant bacteria*. 1–21.

Kumar, S., Pandit, V., Bhattacharyya, K., & Krishnan, V. (2018). AC SC. *Materials Chemistry and Physics*. https://doi.org/10.1016/j.matchemphys.2018.04.113

Kuppusamy, P., Yusoff, M. M., & Maniam, G. P. (2016). Biosynthesis of metallic nanoparticles using plant derivatives and their new avenues in pharmacological applications – An updated report. *Saudi Pharmaceutical Journal*, *24*(4), 473–484. https://doi.org /10.1016/j.jsps.2014.11.013

Lemecho, B. A., Sabir, F. K., Andoshe, D. M., Gultom, N. S., Kuo, D., Chen, X., Mulugeta, E., Desissa, T. D., & Zelekew, O. A. (2022). *Biogenic Synthesis of Cu-Doped ZnO Photo catalyst for the Removal of Organic Dye*. *2022*.

Length, F. (2006). *Is Vernonia amygdalina hepatotoxic or hepatoprotective ? Response from biochemical and toxicity studies in rats*. *5*(September), 1648–1651.

Machovsky, M., Kuritka, I., & Kozakova, Z. (2012). Microwave assisted synthesis of nanost ructured Fe 3 O 4 / ZnO microparticles. *Materials Letters*, *86*, 136–138. https:// doi. org/10.1016/j.matlet.2012.07.038

Makarov, V. V, Love, A. J., Sinitsyna, O. V, Makarova, S. S., & Yaminsky, I. V. (2014). *“ Green ” Nanotechnologies : Synthesis of Metal Nanoparticles Using Plants*. *6*(20), 35-44.

Mohanan, A., Sankar, V., Rahdar, A., Joseph, J., Sadeghfar, F., A, R. A., Rajesh, K., & Kyzas, G. Z. (2020). Green synthesis and characterization of zinc oxide nanoparticles with antibacterial and antifungal activity. *Journal of Molecular Structure*, *1211*, 128107. https://doi.org/10.1016/j.molstruc.2020.128107

Mousavi, S. M., Hashemi, S. A., Zarei, M., Bahrani, S., Savardashtaki, A., Esmaeili, H., Lai, C. W., Mazraedoost, S., Abassi, M., & Ramavandi, B. (2020). Data on cytotoxic and antibacterial activity of synthesized Fe3O4 nanoparticles using Malva sylvestris. *Data in Brief*, *28*, 104929. https://doi.org /10.10 16 /j.dib.2019.104929

Ocimum, L., Nair, S. K. P., Ganesan, K., Azalewor, H. G., & Letha, N. (2016). *Preliminary Phytochemical Screening and In vitro Antioxidant Activity of Ethiopian Indigenous Medicinal Plants , Ocimum lamiifolium Hochst . ex International Journal of Pharmaceutical Sciences and Drug Research CODEN ( USA ): IJPSPP Preliminary Phytochemical Screening and In vitro Antioxidant Activity of Ethiopian Indigenous Medicinal Plants , Ocimum lamiifolium Hochst . ex Benth and Ocimum basilicum L . February*. https://doi.org /10.25004 /IJP SDR.2016.080105

Paper, R., Sabri, M. A., Umer, A., Awan, G. H., Hassan, M. F., & Hasnain, A. (2016). *Selection of Suitable Biological Method for the Synthesis of Silver Nanoparticles Regular Paper*. 1–20. https://doi.org/10.5772/62644

Parveen, K., Banse, V., & Ledwani, L. (2016). *Green Synthesis of Nanoparticles : Their Advantages and Disadvantages*. *020048*. https://doi.org/ 10.1063/ 1.49 45168

Pramanik, K., Thatoi, H., & Patra, J. K. (2016). Photo-mediated green synthesis of silver and zinc oxide nanoparticles using aqueous extracts of two mangrove plant species, Heritiera fomes and Sonneratia apetala and investigation of their biomedical applications. *JPB*. https://doi.org/10.1016/j.jphotobiol.2016.07.029

Rafique, M., Tahir, R., Gillani, S. S. A., Tahir, M. B., Shakil, M., Abdellahi, M. O., Rafique, M., Tahir, R., Gillani, S. S. A., Tahir, M. B., & Shakil, M. (2020). Plant-mediated green synthesis of zinc oxide nanoparticles from Syzygium Cumini for seed germination and wastewater purification. *International Journal of Environmental Analytical Chemistry*, *00*(00), 1–16. https://doi.org/ 10.1080/ 03067319.2020.1715379

Roychowdhury, A., Pati, S. P., Mishra, A. K., Kumar, S., & Das, D. (2013). Journal

of Physics and Chemistry of Solids Magnetically addressable fluorescent Fe 3 O 4 / ZnO nanocomposites : Structural , optical and magnetization studies. *Journal of Physical and Chemistry of Solids*, *74*(6), 811–818. htt ps ://doi .org /10.1016 /j.jpcs.2013.01.012

Singh, I. H. N. B. (2026). Green synthesis of nanoparticles and its potential application. *Biotechnology Letters*, *38*(4), 545–560. https://doi.org /10.1007/s 10529-015-2026-7

Singh, P., Kim, Y., Zhang, D., & Yang, D. (2016). Biological Synthesis of Nanop arti cles from Plants and Microorganisms. *Trends in Biotechnology*, *34*(7), 588–599. http s://doi.org/10.1016/j.tibtech.2016.02.006

Sirelkhatim, A., Mahmud, S., & Seeni, A. (2015a). Review on Zinc Oxide Nanopar ticles : Antibacterial Activity and Toxicity Mechanism. *Nano-Micro Letters*. https:// doi.or g/10.1007/s40820-015-0040-x

Sirelkhatim, A., Mahmud, S., & Seeni, A. (2015b). Review on Zinc Oxide Nanop articles : Antibacterial Activity and Toxicity Mechanism. *Nano-Micro Letters*, *7*, 219–242. https://doi.org/10.1007/s40820-015-0040-x

Soliman, N. K., & Moustafa, A. F. (2020). Industrial solid waste for heavy metals adsorption features and challenges; a review. *Journal of Materials Research and Technology*, *9*(5), 10235–10253. https://doi.org/10.1016/j.jmrt.2020.07.045

Taha Yassin, M., Al-Otibi, F. O., & Al–Askar, A. A. (2024). Green synthesis, charac terization and antimicrobial activity of iron oxide nanoparticles with tigecycline against multidrug resistant bacterial strains. *Journal of King Saud University - Science*, *36*(4), 103131. https://doi.org/10.1016/j.jksus.2024.103131

Tippayawat, P., Phromviyo, N., & Boueroy, P. (2016). *Green synthesis of silver nanoparticles in aloe vera plant extract prepared by a hydrothermal method and their synergistic antibacterial activity*. 1–15. https://doi.org/10.7717/peerj.2589

Tripathy, N., & Kim, D. H. (2018). Metal oxide modified ZnO nanomaterials for biosensor applications. *Nano Convergence*. https://doi.org/10.1186/s40580-018-0159-9

Uikey, P. (2016). *REVIEW OF ZINC OXIDE ( ZNO ) NANOPARTICLES APPLICAT IONS AND*. *21*(2), 239–242.

Ulya, H. N., & Taufiq, A. (n.d.). *Comparative Structural Properties of Nanosized ZnO/Fe 3O 4 Composites Prepared by Sonochemical and Sol-Gel Methods Comparative Structural Properties of Nanosized ZnO / Fe 3 O 4 Composites Prepared by Sonochemical and Sol-Gel Methods*. https://doi.org/10.1088/1755-1315/276/1/012059